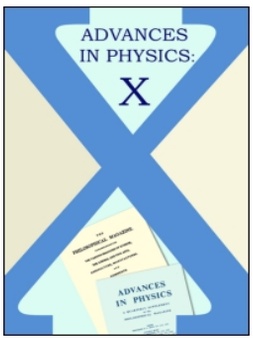

Advances in Physics: X

ISSN: (Print) 2374-6149 (Online) Journal homepage: http://www.tandfonline.com/loi/tapx20

# Helicon high-density plasma sources: physics and applications

Shunjiro Shinohara

**To cite this article:** Shunjiro Shinohara (2018) Helicon high-density plasma sources: physics and applications, Advances in Physics: X, 3:1, 1420424

**To link to this article:** https://doi.org/10.1080/23746149.2017.1420424



Published online: 18 Jan 2018.

ADVANCES IN PHYSICS: X, 2018
VOL. 3, NO. 1, 1420424
https://doi.org/10.1080/23746149.2017.1420424

Taylor & Francis
Taylor & Francis Group

REVIEW ARTICLE

OPEN ACCESS Check for updates

# Helicon high-density plasma sources: physics and applications

Shunjiro Shinohara

Division of Advanced Mechanical Systems Engineering, Institute of Engineering, Tokyo University of Agriculture and Technology, Tokyo, Japan

**ABSTRACT**

Helicon high-density (up to ~$10^{13}$ $cm^{-3}$) plasma sources using a radio frequency wave in the presence of a magnetic field under a low pressure are very promising for various application fields owing to the flexibility of external operational parameters. In addition, these sources have interesting inherent characteristics. Herein, the basic features of helicon wave plasmas including production mechanisms are briefly described, focusing on some similarities to other fields. Examples of specific helicon sources are also introduced. Then, an extensive variety of applications ranging from fundamental to practical applications, which are very influential for further development in each field, are introduced, emphasizing crucial points.

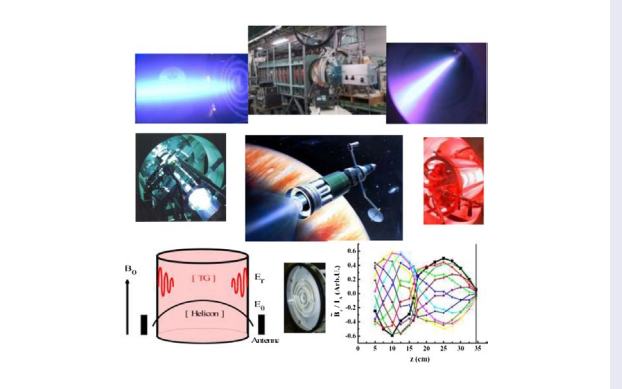


**ARTICLE HISTORY**
Received 19 July 2017
Accepted 18 December 2017

**KEYWORDS**
Helicon; high-density plasma; rf; application

**PACS**
52.50.Qt Plasma heating by radio-frequency fields; ICR, ICP, helicons; 52.50.Dg Plasma sources; 52.35.Hr Electromagnetic waves; 52.35.Mw Non-linear phenomena: waves, wave propagation, and other interactions; 52.75.Di Ion and plasma propulsion; 52.77.-j Plasma applications

**CONTACT** Shunjiro Shinohara sshinoha@cc.tuat.ac.jp

## 1. Introduction

Plasma can exhibit many complex but interesting non-linear behaviors, and self-organized structural formation, which is determined by a balance between stabilizing and destabilizing forces, can occasionally be found in plasma. The clarification of various plasma characteristics leads to the understanding of fundamental concepts, which can be shared and interconnected among many fields, leading to further advancement and development.

Plasmas can be found on earth and in space. They have various forms and behaviors, and advances in plasma science have revealed many application fields, such as energy, nanotechnology/materials, information/telecommunication, environment, space, and biotechnology, which utilize light, heat, electricity and magnetism, dynamics, chemical reactions, and fission reactions (see also Figure 8, shown later). In order to understand these intriguing behaviors physically or to utilize them in many novel application fields, developing a useful plasma source suited to the corresponding field is indispensable and crucial. Target plasma parameters are also governed by a balance between production and loss terms.

Plasmas with a high electron density $n_e$ but low electron and ion temperatures, $T_e$ and $T_i$, respectively, having a low fill pressure $P_f$ discharge are useful and important for practical plasma sources. Among them, Helicon Plasma (HP) sources using Helicon Waves (HW) [1–8], which were first observed by Lehane and Thonemann [9], are very promising for multiple purposes ranging from fundamental to application fields because they can generate plasmas having $n_e \sim 10^{13}$ cm$^{-3}$ with an input power $P_{inp}$ less than several kW at radio frequency (rf) in the presence of a magnetic field. Furthermore, a dense HP, with a typical ionization degree ranging from a few % up to several tens of %, can be easily obtained over a wide, flexible range of external operational parameters under a current-free condition. Thus, no current-driven instabilities can be found: the axial magnetic field $B_0$ in cylindrical geometry typically ranges from a few tens of G to kG with various magnetic field configurations such as uniform, convergent, and divergent fields. The excitation frequency *f,* typically between a few to several tens of MHz when using a noble gas such as argon, lies between the ion and electron cyclotron frequencies, $f_{ci}$ and $f_{ce}$, respectively, with $P_f$ ranging from ~ 0.1 to several Pa. Note that a HW plasma production scheme with these wide ranges of frequency and magnetic field is advantageous compared to, e.g. the Electron Cyclotron Resonance (ECR) plasma production scheme [10–12], for which $f$ must be equal to $f_{ce}$ at a certain position under a divergent magnetic field (so-called the magnetic beach concept) if a wave with a right-hand circular polarization (R wave) is excited from an end of a cylindrical chamber.

Therefore, this advantageous dense source has various applications, such as industrial plasma processing; nuclear fusion; and, recently, plasma thrusters, in addition to basic fields, which will be described later. Here, a HW used to produce HP is categorized as a bounded wave in a whistler wave [10–13] with a wide range

of frequencies $f_{ci} << f << f_{ce}$, as mentioned previously, and with both right- and left-hand (L wave) circular polarization. It is well known that this whistler wave is produced by lightning strokes and can propagate with an audio frequency along the Earth's magnetic field.

The remainder of this paper is organized as follows. In Section 2, basic interesting characteristics of HP, which shows self-structural, standing-wave patterns under flexible external parameters, are described with an emphasis on a brief discussion of high-efficiency plasma production. Some examples of featured helicon sources are also introduced, which may be useful for potential future applications. Next, extensive applications utilizing helicon sources, including fundamental fields (Section 3.1), plasma thruster field (Section 3.2), and practical fields (Section 3.3), are introduced, emphasizing the potential for future utilization. Finally, conclusions on useful helicon high-density sources as well as directions for future works are presented in Section 4.

## 2. Basic features of HW plasma

In rf discharges, an oscillating electric field is excited by, e.g. an external antenna, causing plasma production in an ionization process by accelerating and heating electrons. In an Inductively Coupled Plasma (ICP) [12,14,15], where the excited wave is categorized as a non-propagating one, the external oscillating field is cancelled because the electric conductivity $\sigma$ in a plasma is high. Therefore, only skin heating can be expected within a thin layer up to a depth on the order of $c/\omega_{pe}$ from the plasma surface, where $c$ is the velocity of light and $\omega_{pe}$ is the electron plasma angular frequency. On the other hand, since HW is a propagating wave, it can propagate into the plasma with wave absorption, contributing to global plasma production.

### 2.1. Dispersion relation and wave structure of HW

Here, the dispersion relation of HW is briefly described with some discussions including wave structures. In the presence of an axial magnetic field $B_0$ in a cylindrical geometry with a uniform electron density $n_{e0}$, consider two of Maxwell's equations: $\nabla \times \mathbf{B} = \mu_0 \mathbf{j}$, where $\mathbf{B}$ is the wave magnetic field, $\mathbf{j}$ is the current density, $\mu_0$ is the permeability in vacuum, and displacement current is neglected in this frequency range, and $\nabla \times \mathbf{E} = -\partial \mathbf{B}/\partial t$, where $\mathbf{E}$ is the electric field of the wave. Using these Maxwell's equations, the following relations can be derived in SI units:

$$\nabla \times \mathbf{B} = \alpha \mathbf{B}, \tag{1}$$

$$\alpha = \frac{\omega}{k_{//}} \frac{\omega_{pe}^2}{\omega_{ce} c^2}. \tag{2}$$

Here, the HW field is expressed as being proportional to exp (i $m\,\theta$ + i $k_{//}\,z$ – i $\omega\,t$), and $\omega$, $k_{//}$, $\omega_{pe}$, and $\omega_{ce}$ denote the wave angular frequency, parallel wavenumber along the axis ($B_0$ direction), electron plasma angular frequency, and electron cyclotron angular frequency, respectively. In deriving these equations, we have assumed that a plasma current is carried by only electrons in this frequency range in the form of an $\mathbf{E} \times \mathbf{B}$ drift motion of the guiding center: $\mathbf{j}_\perp = e\,n_{e0}\,\mathbf{E} \times \mathbf{B}_0 \,/\, B_0^2$, where $\mathbf{j}_\perp$ is the perpendicular component of current density with respect to $\mathbf{B}_0$ (static axial field) and $\mathbf{E}$ directions, and e is the elementary charge. In addition, the plasma resistivity $\eta = 1/\sigma$ is neglected, and its inclusion effect will be discussed later. Note that Equation (1) shows that $\mathbf{B}$ and $\mathbf{J}$ are parallel to each other with the relation $\mathbf{J} = (\alpha/\mu_0)\,\mathbf{B}$, which is so-called a force-free (no Lorentz force) condition, since $\nabla \times \mathbf{B} = \mu_0\,\mathbf{j}$ is satisfied in this case.

Curling Equation (1), we can obtain:

$$\nabla^2 \mathbf{B} + \alpha^2\,\mathbf{B} = 0\,. \tag{3}$$

The solutions of this equation have the form of Bessel functions [16]: boundary conditions require that a solution is finite at $r = 0$ and, e.g. a radial component of current density $j_r = 0$ at an inner insulator surface (discharge tube) of $r = a$, which imposes a discrete perpendicular wavenumber $k$. Thus, a standing wave pattern is formed in the radial direction. Since the HW satisfies the whistler wave dispersion relation, HW is also called a bounded whistler wave, as mentioned previously. Here, $k_\perp$ satisfies the relation $\alpha^2 = k_{//}^2 + k_\perp^2$ [16].

It is interesting to see that this Bessel function solution is similar to the Reversed Field Pinch (RFP) plasma [17] of magnetic nuclear fusion machines, in which a self-organized structure (toroidal magnetic field reverses near the plasma edge, in contrast to the axis) can be observed with magnetic fields that has a form of Bessel functions. This form can be explained by the idea that the RFP configuration works toward a minimum magnetic energy state in MagnetoHydroDynamics (MHD), keeping the helicity $\mathbf{A}\cdot\mathbf{B}$ constant, where $\mathbf{A}$ is the vector potential [18]. This idea can also be applied to a magnetic loop reconnection in the solar corona [19].

Figure 1 shows the dispersion relation of this HW with uniform electron density and the $m = 0$ mode from Equation (3), considering an insulating boundary condition at $r = a$, where $a$ is the plasma radius and we take the fundamental radial mode. With increasing $k_{//}$ and/or decreasing $a$, the value of $f\,n_e/B_0$ increases ($B = B_0$ in this figure). In other words, once external parameters such as $a$, $f$, and $B_0$ are chosen, we can establish a relation between $n_e$ and $k_{//}$. Note that in the case of a peaked radial density profile compared to a uniform one, the effective radius $a$ becomes smaller.

The inclusion of a collision frequency $\nu$ corresponding to, e.g. electron–ion and electron-neutral collisions, yields the following set of two equations [16], which is similar to Equation (1):

$$\nabla \times \mathbf{B}_{1,2} = \beta_{1,2}\,\mathbf{B}_{1,2}\,. \tag{4}$$

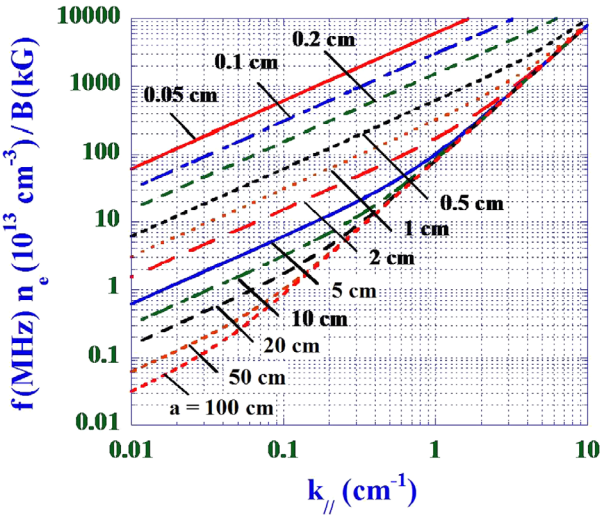


**Figure 1.** Dispersion relation of helicon wave with the $m = 0$ mode in the ($f\,n_e$/B, $k_{//}$) plane for varying $a$.

Here, $\beta_{1,2} = [1 \mp (1 - 4\alpha\gamma)^{1/2}]/(2\gamma)$ and $\gamma = (\omega + i\nu)/(k_{//}\omega_{ce})$ and complex values $\beta_1$ and $\beta_2$ correspond to an HW with a low $k_\perp$ value and a Trivelpiece-Gould (TG) wave with a high $k_\perp$ value, respectively, the characteristics and plasma production mechanism of which will be described in the next subsection 2.2. Note that the form of Equation (4) is similar to the form obtained with the double Beltrami condition, describing magnetic fields and velocities in high-velocity flow and high-beta plasma with two fluids [20].

As mentioned previously, HW is constrained in the radial direction with the form of a standing wave pattern, so-called a bounded whistler wave, so that discrete radial mode numbers defined as an integer $n$ exist in principle. Each mode number has a separate value of $k_\perp$ as well as a different $k_{//}$ value from the HW dispersion relation, $\alpha^2 = k_{//}^2 + k_\perp^2$, as mentioned previously. Therefore, from wave measurements, complex wave behaviors with mixed modes can be observed in the radial and axial (beating wave pattern) directions [21–24]. In the extreme case with high density and large radius, higher radial modes up to $n \sim 8$ were suggested from the HW dispersion relation using internal antennas [25]. On the other hand, if the axial length is small with the same order of wavelength of HW, axial standing wave patterns imposed by axial boundary conditions in small [26] and large diameters [24,27] can be found. Depending on these conditions, the axial mode number $n_a$ (number of wavelengths in an axial plasma length) differs: its values are $(1 + l)/2$, $(1 + l)/2$, and $(1 + 2\,l)/4$, respectively, for the cases of insulation (one end boundary)-insulation (the other end boundary), metal-metal, and insulation-metal, where $l$ is an integer not less than 0, as long as surface waves near boundaries can be neglected [24].

Concerning a selective excitation of the azimuthal mode number $m$, some examples of various rf antenna configurations are shown in Figure 2 [6]: (a) single or multi loops for the $m = 0$ mode; (b) the Boswell type for both $m = \pm 1$ modes; (c) saddle type for both $m = \pm 1$ modes; (d) the Nagoya type III antenna, which was used for additional heating, i.e. ion cyclotron heating [28] in the field of nuclear fusion, for the $m = 1$ or $-1$ mode depending on the rf phase between leg currents; (e) the half or full helical type for the $m = 1$ or $-1$ mode depending on the direction of the axial magnetic field and/or twisting direction; and (f) the spiral type for $m = 0$ excitation [29,30], which is useful for increasing the plasma radius. Among them, except for the case of (f), where the antenna is located at the end of the chamber (outside) through an insulation window, antennas in the cases of (a)–(e) are wound around the outer, lateral surface of an insulation tube.

Here, the $m = 1$ mode is mostly employed instead of the $m = -1$ mode [31,32] because it usually yields better plasma performance, in addition to the use of the $m = 0$ mode. However, the reason for the better plasma performance with the $m = 1$ mode is not yet been understood physically. Note that negative and positive mode numbers can propagate with equal amplitudes in nearly unbounded and uniform plasmas with $a = 75$ cm (excitation loop diameter is 4 cm) [33], under low field ($B_0 \sim 5$ G) and low $n_e$ ($10^{11}$ cm$^{-3}$) conditions with $f/f_{ce} = 0.357$. The use of the $m = 2$ mode was also tested [34,35], and plasma performance was compared directly between various modes from $m = 0$–2 with a proper choice of antenna feeder parts of a segmented multi-loop antenna [36]. The control of the axial wavenumber $k_{//}$ spectrum has been executed to investigate plasma performance, considering the HW dispersion relation, using antennas at different axial locations with a current phase difference [23,25,37,38].

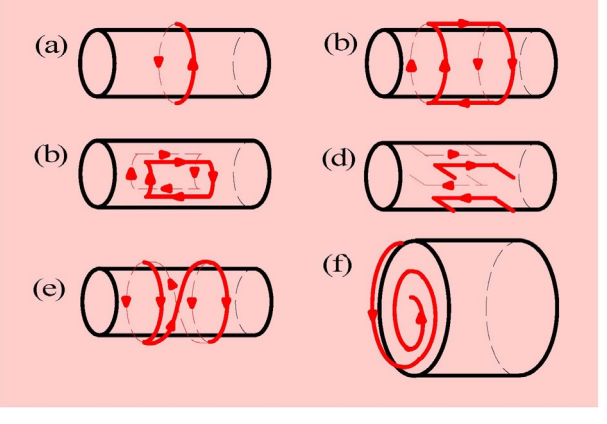


**Figure 2.** Various antennas to excite HW [6].

### 2.2. Highly efficient plasma production and its mechanism

Although HP with $n_e \sim 10^{13}$ cm$^{-3}$ can be easily obtained with a very high efficiency and is utilized in many ways as described in Section 3, there have been many disputes and discussions regarding the high-density plasma production mechanism. Here, we describe HP production with a high efficiency, followed by a discussion on this mechanism.

Figure 3 [39] shows an example of $n_e$ as a function of $P_{inp}$ using the Large Helicon Plasma Device (LHPD) [40,41] developed by our group at the Institute of Space and Astronautical Science (ISAS), Japan Aerospace eXploration Agency (JAXA). This machine has an axial length $L$ of up to 486 cm (in this figure, $L$ is shortened to 81 cm in the presence of a termination plate) with an Inner Diameter (I.D.) of 73.8 cm. From this figure, an increase in $P_{inp}$ results in the increase of $n_e$. From low $P_{inp}$ region where $n_e$ is on the order of $10^9$ cm$^{-3}$, which is a typical mode of Capacitively Coupled Plasma (CCP) [12], HP can be obtained through ICP with a clear density jump, which is a typical behavior from ICP to high-density HP (see also Figure 8 in [42], where jumps of $n_e$ and Ar II intensity can be found from CCP to ICP and from ICP to HW). Note that it is very useful to initiate a plasma with a very low $P_{inp}$ less than 1 W (not shown), which corresponds to an average power density on the order of μW/m$^3$. It is also shown from this figure that the minimum $P_{inp}$ required for this jump from ICP to HP density increased with increasing static magnetic field (axial component) near the antenna $B_a$, which is controlled by the coil current.

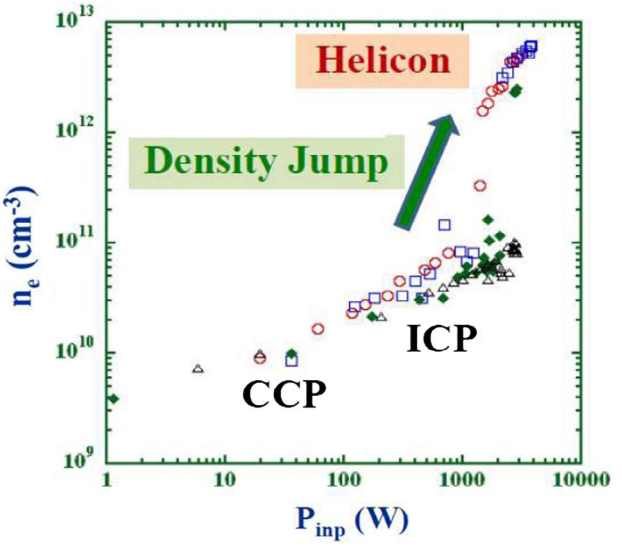


**Figure 3.** $n_e$ as a function of $P_{inp}$ for varying magnetic field near the antenna, $B_a$ [39].
Notes: The coil current near the antenna to control $B_a$: $I_c$ = 20, 40, 60, and 80 A in the cases of red open circles, blue open boxes, green closed diamonds, and black open triangles, respectively.

Figure 4 shows the particle production efficiency, i.e. the relationship between $N_e/P_{inp}$ and $a^2$, where $N_e$ is the total number of electrons in a whole plasma region. A good agreement was obtained between experiments and the theoretical upper limit, indicated by the dotted line, with an enhancement diffusion factor ~3 [43] (the case where radial diffusion is dominant over axial diffusion) over a very wide range of plasma radius $a$ from 0.05 to 38 cm. Data with red closed circles were taken by our group, and our spiral antennas were used for $a$ greater than ~10 cm to achieve better plasma performance than the other antenna types shown in Figure 2. An internal antenna wound around a plasma shows a poor efficiency in Figure 4. Here, studies on HW excitation have been recently conducted with a small $a$ less than 1–2 cm, in addition to the cases of $a$ = 0.05 cm (no magnetic field) and 0.15 cm [44]. However, direct electrostatic probe measurements have not been performed with $a$ less than 0.15 cm [44], since the probe size is comparable to the plasma diameter, making the measurements difficult. Instead, plasma density was estimated from data outside the small radial region and from plasma light intensity ratio measurements based on the collisional radiative (CR) model [45,46]. In summary, helicon sources are one of the most promising types of sources for high particle production efficiency and can be applied in many ways.

Next, we describe a highly efficient HP production mechanism, which has been disputed for close to three decades. Basically, there are several candidates accounting for this high-density plasma production: e.g. (i) electron–ion $\nu_{ei}$ and electron-neutral $\nu_{en}$ collisional dampings [16]; (ii) electron Landau damping [10,16] along with a near-field effect to accelerate electrons; (iii) mode conversion process, which is a universal, general character in plasma waves [10,11] first proposed by Shamrai in the HW regime [47]. Here, this process is from HW to TG waves, which is then damped strongly in a plasma due to a small radial wavelength, as

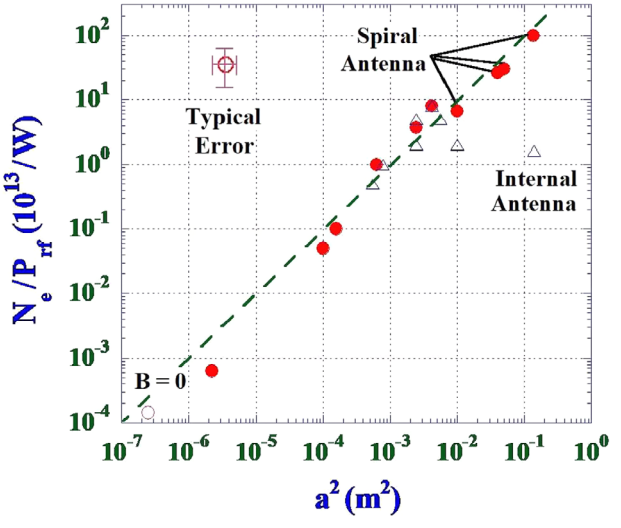


**Figure 4.** Relationship between $N_e/P_{inp}$ and $a^2$ for different helicon sources.

was mentioned in Equation (4); (iv) electrostatic ion sound instability/turbulence (parametric decay of HW) [48–50]; and (v) surface-type helicon mode [51].

Now, we consider the first three candidates (i)–(iii). Since (i) collisional dampings are weak except for high-density conditions, (ii) the kinetic effect of Landau damping was first considered: the thermal electron velocity is comparable to the phase velocity of a wave to accept a plasma-wave interaction [16,52]. However, it was discarded because of the insufficient number of fast electrons observed [53] to account for the main ionization. This can be also understood from the following discussion on energy [47]. We express wave magnetic and electric fields and particle energy as $W_B$, $W_E$, and $T$, respectively. Then, $T = (\alpha\, c/\omega_{pe})^2\, W_B << W_B$ as $\alpha\, c/\omega_{pe} << 1$ for HW, and $W_E \sim T\,(\omega_{ce}/\omega_{pe})^2 << T$ under typical experimental conditions. Thus, a decay of total energy $W_T = W_B + T + W_E$ cannot be explained by a decay of $T$ alone.

Then, (iii) a fluid view of mode conversion was considered. Since $\alpha\, c/\omega_{pe} >> 1$ for TG waves, $T >> W_B$, leading to a dominant role of $T$ concerning the decay of $W_T$ [47]. This TG mode with small radial wavelength has strong collisional damping, which can explain efficient plasma production. Here, in a cold plasma dispersion relation, we can generally have two solutions [10–12]: one has a small wavenumber (HW: fast phase velocity), and the other has a large wavenumber (TG wave: slow phase velocity), which was also discussed in Equation (4).

Figure 5 [6] shows a schematic concept of the mode conversion processes [47] in the case of (a) non-uniform (bulk mode conversion) and (b) uniform (surface mode conversion) radial electron density profiles: (a) At a certain radial point, excited HW from a plasma surface, tunneling through an evanescent area between the plasma boundary of $r = a$ and $r_{low}$, converts to a TG wave at $r = r_{up}$ with the same $k_\perp$ value of HW, and this TG wave damps strongly due to the increasing $k_\perp$ with a backward propagation toward the outer radial direction. In the experiment, there is a wide spectrum of $k_{//}$, leading to different positions of merging between two waves; thus, bulk plasma production can be expected. (b) At the plasma boundary, regardless of materials (conducting and non-conducting), the radial component of current density is zero, which leads to a radial electric field $|E_r| \sim (\omega_{ce}/\omega)\,|E_\theta| >> |E_\theta|$ ($E_\theta$: azimuthal electric field). Then, the excitation of long-wavelength HW with the $E_\theta$ component inevitably induces the short-wavelength TG wave, which damps strongly near the plasma surface. Note that, in the case of a higher magnetic field where $f < f_{LH}$ is satisfied [$f_{LH}$: lower hybrid (LH) frequency $\sim (f_{ci} f_{ce})^{0.5}$], two lines of both waves are not connected, in contrast to the case in Figure 5 with $f > f_{LH}$.

After the recognition of the mode conversion process into a TG wave, many calculations based on this process have been reported, e.g. [54,55] on HP performance and wave structures excited by many types of antenna in uniform and non-uniform density profiles. Simulation codes have been also developed, such as ANTENA2 [56,57]; HELIC [58–60], which is an open-source code [61]; and, more recently, SPIREs [62] and ADAMANT [63].

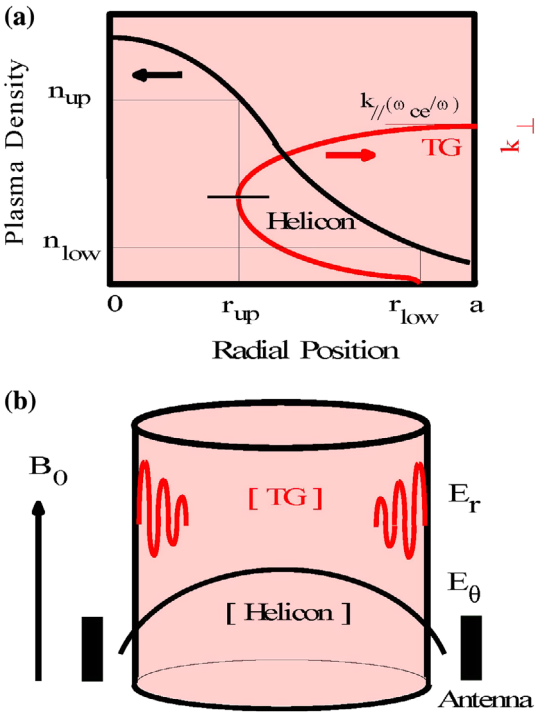


**Figure 5.** Mode conversion model from HW to TG wave [6].

Note that the physical picture of the mode conversion shown in Figure 5(a) is similar to the Ion Cyclotron Range of Frequency (ICRF) heating in fusion machines: there is a mode conversion [64] from Fast Magnetosonic Waves (FMW) with a longer wavelength to ion Bernstein waves (IBW) with a shorter wavelength near the ion–ion hybrid resonance layer with more than two plasma species, and direct measurements of both waves were executed by magnetic probes and the 2-mm microwave scattering method [65]. Generally, in a cold plasma, for waves with a fixed $k_{//}$, we have a quadratic equation with respect to $k_{\perp}{}^2$ [10–12], and the two solutions of the quadratic equation correspond to high and low $k_{\perp}{}^2$ values. Depending on parameters, two lines in ($n_e$, $k_{\perp}{}^2$) space merge on a certain point (so-called 'bifurcation,' but no unstable modes can be found in this case), where the mode conversion occurs.

Experimentally, because of a very short wavelength, it is difficult to observe the TG wave using, e.g. electric, magnetic, and current probes in addition to the Laser-Induced Fluorescence (LIF) method. In the case of an indirect measurement, the antenna resistance, excited magnetic field profile, and density jump behaviors were consistent with calculation, which includes the effect of the TG wave, for various operation parameters [66,67]. Under a low density (on the order of $10^{11}$ cm$^{-3}$) and a low magnetic field (a few tens of G), TG waves were observed directly by measuring rf magnetic fields [68] and rf current densities [69].

Although it is now widely accepted that the TG wave can play a dominant role in high-density HP production, its interpretation can be different with fluid and Finite-Difference Time-Domain (FDTD) calculations in a non-uniform density profile [70], depending on $\nu/\omega$ ($\nu=\nu_{ei}+\nu_{en}$). With increasing $\nu/\omega$, owing to the separation of lines of HW and TG waves in the $k_\perp$ and $r$ plane [see Figure 5(a)], more HW energy directly dissipates and heats the plasma, and surface mode conversion becomes dominant compared to the bulk mode conversion. This must be further investigated. Note that studies on the dynamic formation of the excited helicon wave structure and the estimation of wave-energy flux distribution were attempted to understand the HW phenomena [71,72].

### 2.3. Examples of developed HP sources and their characteristics

#### 2.3.1. Various HP sources with different sizes and machine geometries

Here, we show various HP sources developed with different objectives, and helicon sources with a torus geometry will be described in Section 3.1.3. Some typical linear machine characteristics are summarized in Ref. [41], which was published in 2004. The first large helicon machine built was named the Waves On Magnetized Beams And Turbulence (WOMBAT) machine [73,74], which was 20 cm in diameter $D$ and 50 cm in axial length $L$, and it was connected to a large chamber with $D$ = 90 cm and $L$ = 250 cm to perform many physical experiments, including interesting mode transitions from CCP to HP through ICP.

Subsequently, various HP sources were developed with a typical $D$ of 5–10 cm. Large machines are as follows: LHPD [40,41,75] with $D$ = 73.8 cm and $L$ = 486 cm, which corresponds to a plasma volume $V$ of 2.1 m$^3$ (the largest volume in the world); a former machine developed by the Archimedes Technology Group [25] with a plasma diameter of 74.8 cm restricted by an rf antenna, which has $L$ = 389 cm and $V$ = 1.7 m$^3$; and a Large Mirror Device (LMD) [30,76] with $D$ = 44.5 cm, $L$ = 170 cm, and $V$ = 0.26 m$^3$. LHPD and LMD utilized spiral-type antennas [29,30], as shown in Figure 2(f), to increase the plasma diameter effectively, with additional advantages such as the easy positioning (installation and removal) of antennas outside a vacuum vessel at the end of a vacuum chamber and the reduction of inductive effect of antennas due to the proximity of an impedance-matching box [39]. On the other hand, large-diameter plasma production is difficult with a low production efficiency if antennas are located around the plasma cylinder [25,77], probably due to an rf penetration problem (first by CCP/ICP mode excitation to enter HP) from the plasma surface into the plasma core [78,79]. Therefore, in the case of internal antenna, a very large rf power of the order of several hundred kW was necessary for large-diameter HP with $n_e \sim 10^{13}$ cm$^{-3}$ [25] (see also Figure 5).

The articulated Large-Area Plasma Helicon Array (ALPHA) [80] with $D$ = 50 cm and $L$ = 400 cm and, later, the Helicon-Cathode (HelCat) combined source [81] were developed using seven independent sources with a plasma

diameter of ~ 43 cm to produce large-diameter and large-volume plasma with good uniformity. However, this trial was difficult to be realized due to, e.g. cross rf coupling between sources and unstable discharges. Using multiple small helicon sources with Permanent Magnets (PMs), a large-area plasma was produced in a 53.3 × 165 $cm^2$ chamber ($L$ = 30 cm) with $n_e < 10^{12}$ $cm^{-3}$ [82].

Medium-sized helicon sources are as follows. The Versatile Instrument for studies on Non-linearity, Electromagnetism, Turbulence, and Applications (VINETA) [83,84] with $D$ = 40 cm (plasma diameter is 10 cm) and $L$ = 450 cm was constructed for studying mode transition behavior, whistler wave excitation, drift wave turbulence, etc., which will be described later. The Controlled Shear Decorrelation eXperiment (CSDX) [85,86] with $D$ = 20 cm (plasma diameter is 10 cm) and $L$ = 300 cm was used to study drift wave turbulence, which will also be described later. The Auburn Linear Experiment for Space Plasma Investigations (ALESPI) [87] with $D$ = 15 cm (plasma diameter less than 10 cm) and $L$ = 250 cm for the study of Alfvén waves takes advantage of a high-density source to reduce the wavelength of this wave. Various HW studies have been executed in a large-volume helicon source HE-L [35] with $D$ = 15 cm and $L$ = 200 cm connected to a larger vacuum chamber with $D$ = 60 cm and $L$ = 100 cm. The hot HELIcon eXperiment (HELIX) with $D$ = 15 cm and $L$ = 157 cm connected with a larger chamber of the Large Experiment on Instabilities and Anisotropies (LEIA) with $D$ = 200 cm and $L$ = 450 cm under a low magnetic field [88,89] was employed to study basic helicon characteristics, including a space-relevant physics study, with an advanced laser-induced fluorescence (LIF) development. There are helicon sources with $D$ = 13 cm and $L$ = 30 cm connected to an expansion chamber of $D$ = 60 cm and $L$ = 120 cm [90], with $D$ = 10 cm and $L$ = 120 cm [91] and with $D$ = 10 cm and $L$ = 35 cm (T-shaped glass tube) [68] for studying HW and TG waves. Other sources have $D$ = 10 cm and $L$ = 175 cm [92], a discharge tube of $D$ = 5 cm and $L$ = 50 cm connected to a vacuum chamber of $D$ = 44.5 cm and $L$ = 170 cm in LMD [37], and a tube of $D$ = 4 cm and $L$ = 130–160 cm [93] for various helicon studies. The Shoji and Sakawa group studied many basic HW studies using a Pyrex source with $D$ ~ 5 cm and $L$ = 60–90 cm, connected to a stainless steel chamber with $D$ = 150 cm and $L$ = 36.5 cm [94,95].

Small helicon sources are as follows. Small helicon sources with $D$ = 2.5 cm [96] and 2 cm [97] were developed for a thruster experiment with miniaturized sizes. Sources with even smaller diameter have been developed using the small helicon device (SHD) [98], with diameter ranging from $D$ = 2 cm to just 0.3 cm [99,100] (now, plasma production with 0.05 cm diameter is possible but without the magnetic field [44]) through $D$ = 0.15, 0.5 and 1 cm, as previously mentioned, although the operation mode may be the magnetized ICP mode. In this device, an excitation frequency $f$ higher than the usual frequency range from several MHz to a few tens of MHz was also utilized, e.g. 50–70, 145, and 435 MHz. Here, according to the dispersion relation (see also Figure 1), $f n_e$ /B is larger when $a$ is smaller; thus, in a fixed range of $n_e$ and B (and $k_{//}$), a higher $f$ may be better. From the viewpoint

of electron excursion length $L_e$ in one rf cycle, a higher $f$ is also desirable in a thin discharge tube. This can be easily understood from a simple equation of motion in the presence of an oscillating electric field E, with $L_e$ expressed as e $E/(m\,\omega^2)$, where $m$ is the mass of the electron and $\omega$ is the angular rf frequency.

In this subsection, we have described various characteristics of helicon sources with different sizes and machine geometries, listing some examples, after introducing basic features of HW plasma in the former subsections. Finally, for information, typical helicon linear sources developed by us along with high-density plasma photos are shown in Figure 6: (a) the largest machine LHPD with photos of argon blue modes, (b) LMD with high-density modes, (c) High-Field Device

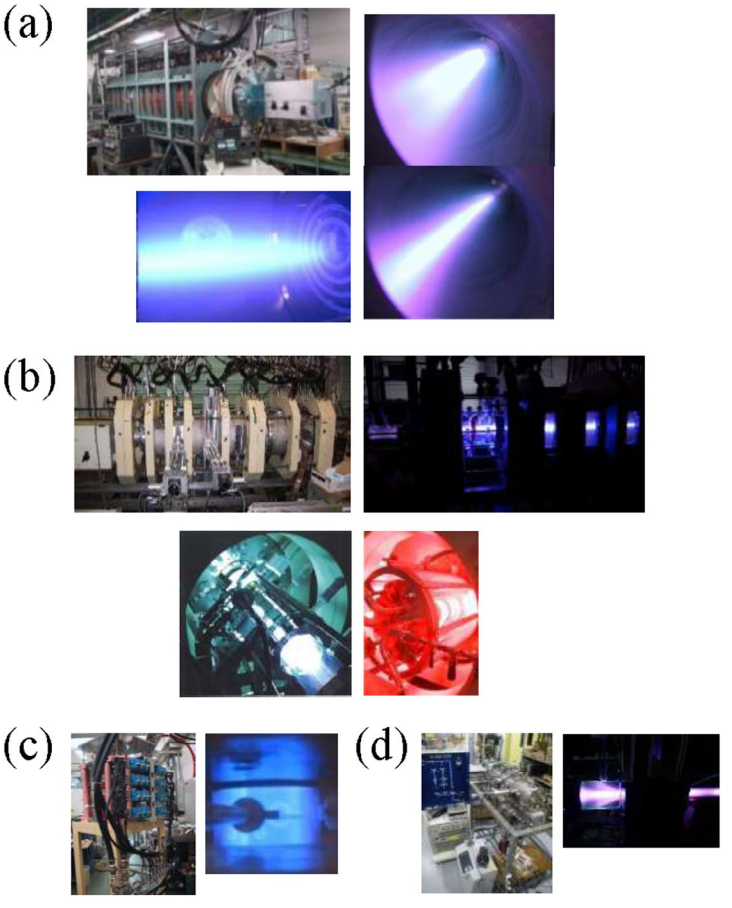


**Figure 6.** Typical helicon sources with photos: (a) the largest machine, LHPD, with argon blue modes [one from a side quartz window, and two from a source region, showing different radial plasma sizes (they look smaller than real ones from a distance owing to optical geometry) by changing the magnetic field configuration]. (b) LMD with high-density modes [right: argon (entire region), left bottom: xenon (source region), and right bottom: neon (source region)], (c) HFD with the argon blue mode (side view), and (d) the smallest machine, SHD, in the presence of the divergent magnetic field (side view).

(HFD) [101] with an argon blue mode, and (d) SHD with a divergent magnetic field.

### 2.3.2. Effect of external parameters on HP behaviors

First, featured HP sources with high- or low-magnetic field operations are introduced, including various magnetic field configurations. High-magnetic field operation has been performed to achieve a higher $n_e$ compared to the operation with a typical field <kG. From the HW dispersion relation of $\alpha^2 = k_{//}^2 + k_{\perp}^2$, as mentioned previously, $n_e$ increases with $B$ while keeping external parameters including $k_{//}$ constant. Needless to say, the high field can reduce radial particle loss, leading to a higher density. The VAriable Specific Impulse Magnetplasma Rocket (VASIMR®) device [102,103], the concept of which is shown in Figure 7 [104], was developed as an advanced plasma thruster (as will be discussed in Section 3.2), using superconducting magnets with the highest field $B$ = 20 kG in a 150 m$^2$ vacuum chamber. Operation up to 10 kG was possible in HFD, where density jumps from ICP to HP was found in low-$B$ operation. However, it was difficult to observe this jump within a limited $P_{rf}$ less than 2.5 kW in a high-$B$ region above 3 kG, and even without jumps, $n_e$ was high on the order of $10^{13}$ cm$^{-3}$, which suggests that the threshold rf power $P_{rf}$ for a density jump generally increases with $B$ from a power balance calculation [105,106]. Operation up to 6 kG with a divergent-magnetic field configuration for a plasma thruster study was possible to show the reduction of cross-field diffusion [107]. On the other hand, low-field operation using helicon sources was also attempted. Even in the case of $B$ = 18 G and 36 G, HW was excited using a spiral antenna [30,76]. Here, a smooth transition without a clear density jump from CCP/ICP to HP was found, which shows the good controllability of density.

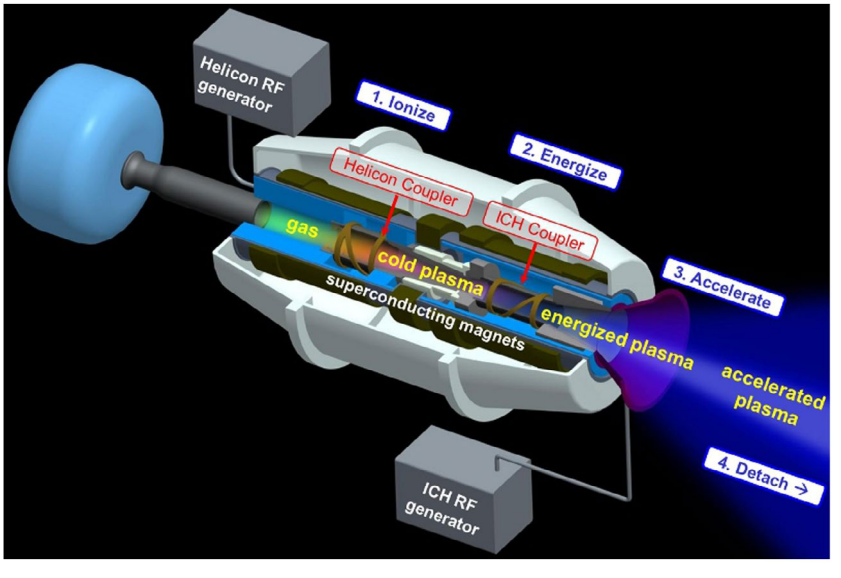


**Figure 7.** Diagram of VASIMR [104].

In addition, a sharp density peak was observed as a function of the magnetic field in the low-field region of a few tens of G [77,108–111]; this phenomenon is still under investigation.

Helicon sources can accept various magnetic field configurations, which are flexible compared to, e.g. ECR plasma sources, as was mentioned in the introduction. Here, experiments under convergent or divergent fields, where the latter is related to a magnetic nozzle in a plasma thruster mentioned later, to control the plasma diameter in addition to propagating wave characteristics are investigated [112]. The cusp of the magnetic field showed interesting behaviors. When the uniform field in the end section changed from a uniform to cusp field by varying the end coil current, $n_e$ increased by a factor of five with a peaked $n_e$ profile [113]. In the presence of cusp or convergent fields in an upward region from the rf antenna using a compact helicon source, $n_e$ increased by several times with a peaked profile [114]. Theoretically, it may be due the change of wave power deposition from a surface to interior regions to enhance the plasma production. Note that the convergent field near the source may produce a ponderomotive force, which can be utilized as a plasma propulsion using an $m = 0$ antenna in a non-uniform $n_e$ profile [39]. Passing through a cusp position, we have investigated wave structures such as tunneling and standing wave patterns with a high radial mode as well as broader $n_e$ profiles (good uniformity of ion saturation current over 27 cm in diameter within ±5% was obtained [115]) by the use of a spiral antenna while changing the position of the cusp field and its strength [116,117]. When the magnetic field is rapidly bent in a downstream region, a standing wave pattern was formed by the presence of a spatially localized change of refractive index [118].

Next, we discuss the effect of a change of rf frequency $f$, especially in a higher frequency range, including the LH resonance regime, on the plasma performance [10,11], considering gas species as a fuel. Normally, the excitation frequency $f$ is 13.56 MHz or $f$ is in the vicinity of this frequency range, and operation with a higher frequency range from ~50 MHz up to ~145 MHz [mostly the Very High Frequency (VHF) range] has been attempted. Here, the objectives of using this higher $f$ are as follows. (1) By increasing $f$, it is important to find threshold parameters such as $P_{inp}$, $P_f$, and $B_0$ [119] for an abrupt density jump from ICP to HP. This investigation may lead to a better control of ion bombardment in plasma processing. (2) Although, in molecular gases, the wavelength of HW using the typical frequency mentioned previously is long on the order of m owing to a lower $n_e$ in the range of $10^{11}$–$10^{12}$ cm$^{-3}$, a higher frequency shows a shorter wavelength from the dispersion relation (see Figure 1 for example), which makes wave analysis easier to perform [120]. (3) It is useful to excite the TG wave directly in this higher frequency range to investigate mode transitions among CCP, ICP, and HP [121]. (4) As was mentioned previously, from the dispersion relation (see Figure 1 for example), to produce a small-diameter plasma, higher frequency operation [99,100,122] is better as long as $k_{//}$ and $n_e$, determined by the experimental $P_{inp}$,

are fixed. As was mentioned, the electron excursion length $L_e$ is smaller at higher $f$, which is also suitable for a small-diameter plasma.

Now, we discuss the effect of LH frequency on plasma performance. In helicon sources, an enhancement of electron density $n_e$ near the LH frequency range was found [123–125] by changing gas species (such as hydrogen, deuterium, helium, nitrogen, neon, and xenon gases as well as argon gas, which is most widely used), excitation frequency $f$, and axial magnetic field $B$. There was an increase of $n_e$ especially near the LH resonance layer position in a plasma, leading to a density profile change. In addition, ion temperature increase was found with $f$ less than 70% of $f_{LH}$ [89]. In these experiments, $n_e$ increases with $B$ and then decreases with $B$ above a certain critical magnetic field $B_{cr}$, showing optimum plasma production. However, it is still an open question [101] whether $B_{cr}$ is close to the field that generally satisfies a lower hybrid frequency (including a Doppler shift effect [124]), and it is difficult to find the phenomena under a high fill pressure condition [39,67,126], where the collisional effect becomes stronger. Here, LH waves are mostly being used in nuclear fusion torus machines, e.g. [127], as a toroidal current drive method instead of ion/electron heating, which was originally aimed at.

Third, a density depletion due to a high ionization degree in the plasma core is discussed, which is an obstacle for entering a higher density regime and affects the plasma transport behavior. By directly inserting a capacitive manometer into a plasma, this decrease of neutral density was ascertained [128,129]: The neutrals pressure decreased by a factor of 2–10, which depended on the initial fill pressure and rf power, and obtained results were consistent with simple diffusion models. The time-dependent behavior of a depleted neutral gas density, reduced by a factor of 10 or more, and its temperature were measured from an absorption profile of the argon line by the use of a tunable diode laser [130]. This depletion was also estimated by LIF and spectroscopy profile measurements through a use of a collisional radiative (CR) model [131] and by Two-photon Absorption Laser Induced Fluorescence (TALIF) [132].

This neutral depletion was discussed in a collisional plasma theoretically, e.g. [133], and an effect of neutral pressure $P_0$ was found to be important in a plasma equilibrium experimentally and theoretically [134,135]. In addition, the decrease of neutral density was found to destabilize the drift wave instabilities by a numerical transport study along with an experiment in which baffle plates and additional vacuum pumps were installed [136,137], and the plasma density profile has been modified by neutral injection in order to achieve a higher thrust performance in a helicon source [138].

## 3. Evolution to extensive application

In this section, we discuss various extensive applications using HP sources in three parts: a fundamental study aiming at future applications in some cases, plasma thrusters as one of the applications, and other practical applications. Note that

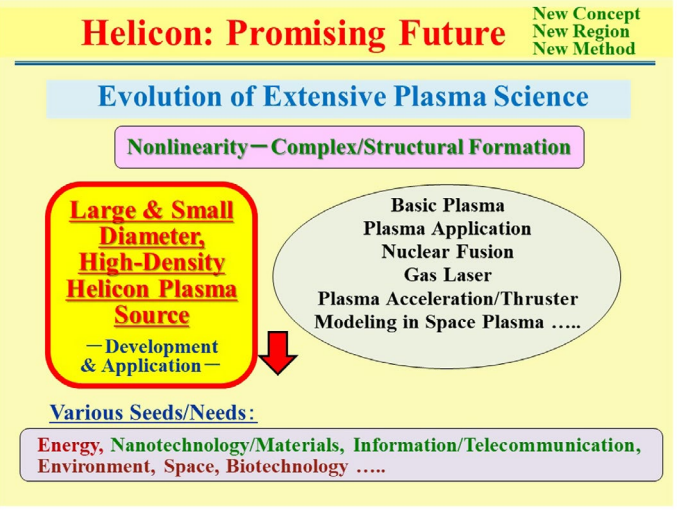


**Figure 8.** Evolution of extensive plasma science using helicon sources.
Note: In various seed/need regions, fields in green are now widely used, while those in red need further development in helicon science.

only some typical practical applications are discussed, since we cannot cover all of them owing to the limited space. Figure 8 shows vast research and application areas including potential future fields in plasma science using helicon sources. This will also be described in Section 4.

### *3.1. Application to fundamental study*

#### *3.1.1. Control/understanding of basic plasma performance*

We show some examples of basic control/understanding of plasma performance using helicon sources. First, we describe the control of radial density profile by three methods: (i) change of magnetic field configurations, (ii) change of antenna radiation field patterns, and (iii) voltage biasing to electrodes in a plasma. These methods are useful for target plasmas in basic and application studies/techniques discussed in subsections 3.2 and 3.3.

(i) A convergent (divergent) magnetic field makes a peaked (broader) radial density profile [40,41,112] since a plasma tends to follow the magnetic field lines, as expected. The cusp field yields a more uniform $n_e$ profile as well as $n_e$ enhancement sometimes, as was mentioned in Section 2.3.2 [113–117]. (ii) By choosing antenna current elements by changing antenna feeder points, antenna radiation patterns could be changed, e.g. rf electric field in a small or large area and/or rf high-voltage point applied in the inner or outer side of spiral antennas, leading to the control of $n_e$ profiles [36,40,41]. (iii) Various combinations of voltage biasing to multi-concentric ring electrodes located at an end of the vacuum chamber in a plasma could also change $n_e$ profiles, e.g. hollow, flat, or peaked ones [139–142]. The effect of a voltage-biased plate, instead of biased rings, on plasma performance

was also investigated, and an asymmetric plasma distribution and its flow were formed, which were consistent with the $\mathbf{E} \times \mathbf{B}$ drift based on the ion Hall parameter $H_i = 2\pi f_{ci} \tau_{in}$, where $\tau_{in}$ is the ion-neutral collision time [143,144].

Going back to the voltage-biased concentric rings, the azimuthal velocity change was controlled by $\mathbf{E} \times \mathbf{B}$ drift, and a strong velocity shear in the radial direction could be formed with associated instabilities: e.g. a change of Mach number of 1 with a distance approximately equal to the ion Larmor radius [141,142,145]. Here, under certain conditions, bistable density transitions, which have similar behaviors of L/H transitions in fusion torus machines with a key of a radial electric field [146], were found and analyzed from the spatio-temporal behaviors [145,147,148]. This biasing can also play an important role to suppress the electrostatic drift instabilities, which are described in subsection 3.1.2.

Here, as an example of application of the voltage-biasing method as well as $n_e$ profile control, we show a mass separation technique in helicon sources by creating a high plasma rotation velocity. Plasma-based mass separation is important for nuclear waste remediation and spent fuel reprocessing, in addition to isotope separation. One way to achieve this is to impose a radial electric field, as was mentioned, by voltage biasing to many concentric electrodes in the presence of an axial magnetic field to create $\mathbf{E} \times \mathbf{B}$ azimuthal plasma rotation, causing trapped (un-trapped) particles with lighter (heavier) mass [149]. Preliminary but encouraging experiments to demonstrate this scheme using mostly noble gases have been performed in low- [150] and high-density [151] operations using helicon sources, although additional experiments are necessary.

### *3.1.2. Various basic plasma characteristics*

First, studies on excited wave characteristics conducted using an induction loop antenna is described, considering its wavelength and the scale length of the radial boundary. Note that these studies are related to the whistler wave and HW mentioned in the introduction. Detailed characteristics of rf waves in the whistler wave range were investigated [152], with the plasma boundary in the intermediate regime between infinite whistler wave propagation and bounded-geometry HW propagation. Here, excited magnetic field amplitudes and phases with three components were measured. Numerical calculation using the Transport Analyzing System for TokamaK/Wave analysis by Finite element method (TASK/WF) code [153] showed good agreement with the observed experimental results, satisfying the dispersion relation and wave structures of helicons in the semi-steady-state condition as well as the dispersion of whistlers with a short-pulsed mode. The excited waves propagated nearly along the magnetic field lines within a small angle of less than 10°. Furthermore, in the low (high) collisional regime, the domination of standing (propagating) waves was found from the wave analysis. These results are consistent with a transition from an unbounded to bounded plasma wave dispersion, which was ascertained by the fact that a short (long) wavelength can be described by the whistler wave theory (by the bounded geometry) [154].

As previously mentioned, helicon wave was also detected in nearly uniform and unbounded plasmas, where excited wave amplitude is determined by the antenna geometry with equal amplitudes observed regardless of polarity of azimuthal mode number [33].

Second, plasma instabilities, the studies of which are important from the viewpoint of a fundamental understanding and the control of plasma confinement, are described. By utilizing a high-density HP with a conventional linear machine, which leads to a high pressure gradient in the radial direction, electrostatic instabilities such as drift wave type ones [10,11] (sometimes the drift wave turbulent state can also be observed) have been investigated intensively and extensively, e.g. [85,86,155–164]. Note that, in the presence of a magnetic field, these instabilities occur inevitably and universally, showing similarities among many fields. For example, in magnetic nuclear fusion plasmas, a critical issue is to obtain an improved plasma confinement, to which detailed understandings of the instabilities can contribute. Here, turbulent helicon plasmas involve many fundamental phenomena such as non-linear mode interaction, structural formation, intermittent behavior, a cascade between large and small scales, sheared and zonal azimuthal flows, and a streamer. Note that, in the stellarator (torsatron type) device TJ-K [165], these studies have been executed, and recently, the dynamics of turbulent suppression by electrode biasing has been attempted, e.g. [166].

Third, high-$\beta$ plasma is discussed. A helicon source can generate a high-density plasma under low magnetic field operation, and thus, a high-$\beta$ plasma condition on the order of unity can be easily achieved. Here, $\beta$ is the ratio of the plasma pressure to the magnetic pressure without a plasma, and high-$\beta$ plasma exhibits non-linear behaviors in various equilibria as well as instabilities with strong diamagnetism. Although a high beta can be obtained only in magnetic fusion fields such as a tokamak and a field reversed configuration (FRC) [167], helicons can have a higher beta region, as observed experimentally. There are a few experiments conducted in a high-$\beta$ region of helicon sources, but the diamagnetism was lower than that expected from the consideration of total pressure balance (sum of plasma pressure and magnetic pressure) [168–170]. It was found that neutral pressure plays an important role in this balance [134]. More detailed data on this equilibrium, along with a study of induced instabilities, are necessary.

Finally, we add a few topics briefly, taking advantage of high-density helicon sources. By utilizing such a source, lasing of the 488-nm Ar II line has been demonstrated [123], showing a larger diameter without discharge electrodes compared to conventional argon-ion gas lasers. Applying helicon sources to an ion source with positive or negative charges is attractive for future particle accelerators, e.g. [171,172], and for neutron generation, which is useful for basic and nuclear fusion reactor studies as well as for detecting land mines. Although neutrons can be generated mostly using a neutron tube or Inertial Electrostatic Confinement (IEC) devices, where the latter was originally conceived as a candidate of a nuclear fusion reactor, a compact neutron source using a helicon source

has been developed with an aim to achieve a higher beam current with a longer life time of operation [173]. Research and Development (R&D) on plasma-facing materials under extreme heat loads is crucial for nuclear fusion reactors such as ITER, e.g. [174], and the future DEMO. The MAGnetized Plasma Interaction Experiment (MAGPIE) [175] with $D = 10$ cm and $P_{rf} = 20$ kW was constructed to test various targets introduced in the presence of a particle (proton) flux greater than $2 \times 10^{22}$ (1/m$^2$s). The Material Plasma Exposure eXperiment (MPEX) [176] is aiming to realize the wall loading condition in a fusion divertor with $D = 13$ cm and to increase the present $P_{rf}$ of 100 kW in addition to other planned heating powers, where the target heat flux is expected to be 10 MW/m$^2$. The International Workshop on Plasma Material Interaction Facilities for Fusion Research (PMIF), which is held every two years, focuses on this important topic.

### 3.1.3. Torus experiment

Here, torus experiments are described, since we have mentioned only linear magnetized machines to produce a cylindrical plasma in Section 2. Many torus helicon studies have been conducted for the purpose of, e.g. studying plasma instabilities excited, pre-ionization/plasma production, discharge cleaning, and current drive in magnetic fusion devices. Here, unless specified, the working gas used is argon.

Simple torus experiments with only toroidal magnetic fields [so called Simple Magnetized Torus (SMT)] have been performed. Coherent structures in turbulent fluctuations were studied, using TEDDI device with major radius $R = 30$ cm and minor radius $a = 10$ cm (limiter radius = 4 cm), using a double half-turn antenna [177]. With a machine of nearly the same size as the above-mentioned device, helicon plasma production and a toroidal current drive of >1 kA with $P_{rf=}1$ kW have been achieved using an $m = 1$ antenna [178]. High-density hydrogen plasma up to $8 \times 10^{12}$ cm$^{-3}$ was produced with $R = 25$ cm and $a = 4$ cm using an $m = 1$, half-saddle antenna [179].

In a stellarator configuration [167], which is one of the magnetized nuclear fusion types, a high-density plasma of $2 \times 10^{13}$ cm$^{-3}$, showing an $m = 1$ HW magnetic structure, was obtained in the toroidal heliac SHEILA with $R = 19$ cm and $a = 3.5$ cm [52]. In the H-1 heliac with $R = 100$ cm and $a = 20$ cm, improved confinement was investigated in a typical electron density of $10^{12}$ cm$^{-3}$ with $P_{rf}$ up to 100 kW using helium, neon, and argon gases in the case of a saddle antenna [180]. Turbulent studies have been performed in TJ-K with $R = 60$ cm and $a = 7$–$10$ cm, which produces a plasma of up to ~$10^{12}$ cm$^{-3}$, using hydrogen, helium, and argon gases in the case of an $m = 1$ antenna [165].

Finally, we mention one example of a clean, pre-ionization helicon source under the 'electrodeless' condition, i.e. no direct contact between a plasma and electrodes, which is important and will be also discussed in Section 3.2. The use of a helicon source has enabled helium plasma breakdown and spheromak [167] formation and sustainment in a nuclear fusion field for the Helicity Injected Torus with Steady Inductive drive (HIT-SI) experiment [181].

### 3.2. Application to plasma thruster using helicon sources

One of the most useful applications of helicon sources attracting increasing interest is plasma thrusters in space. It is well known that plasma-based rocket engines [182,183] are much better than chemical ones because of their higher specific pulse $I_{sp}$ (exhaust velocity divided by gravitational acceleration), which results in better fuel efficiency and reliable long-term operation suitable for, e.g. deep space exploration. However, in most of the present electric (plasma) propulsion systems [182,183], e.g. a Hall thruster, an ion engine, and Magnet-Plasma-Dynamics (MPD), electrodes are in direct contact with a plasma, causing the erosion of electrodes and contamination of plasma. Therefore, the degradation of plasma performance and limited operation lifetime are found.

Here, to overcome this difficulty, the HW plasma production scheme is ideal because of the 'electrodeless' condition (no immersed electrodes) [183], which implies there is no direct contact between a plasma and antennas (electrodes). Therefore, high-density HW plasma is very promising considering the limitations in space, such as limitations in input power [also, e.g. the thrust efficiency $\eta$ (ratio of exhausted kinetic energy per time to input power) and thrust-to-power ratio $F/P_{rf}$ are key parameters], machine size, and weight. Moreover, a neutralizer, which is installed in most of the present thrusters such as the Hall thruster and ion engine, is not necessary, since in a helicon plasma, ions and electrons are exhausted simultaneously. Thus, the system becomes simpler, i.e. it is not necessary to install an electron source.

One remarkable flagship project using a helicon source is the aforementioned VASIMR [102] project, as shown in Figure 7 [104]. This project aims at human space flight to Mars and employs a helicon high-density plasma with a high rf power, which is accelerated by Ion Cyclotron Resonance Heating (ICRH) with a left-hand polarized slow wave scheme, i.e. the so-called magnetic beach [11]. Then, the heated plasma is exhausted through a magnetic nozzle. VX-200 ($P_{rf}$ = 200 kW) [184], developed after the R&D of VX-10, VX-25, VX-50, and VX-100 [185] devices (here, the numerical value denotes the rf power), showed a reduction of ionization cost $E_i$ (energy in units of eV per electron–ion pair production or, in other words, the ratio of the coupled RF power to the total ion current extracted from the system) as well as a high thrust performance using argon gas: maximum values were $E_i$ ~ 80 eV, $I_{sp}$ ~ 4,900 s, plasma thrust $F$ of ~ 6 N, thrust efficiency $\eta$ of ~72%, and $F/P_{rf}$ of ~51 mN/kW. Note that $F$ is inversely proportional to $I_{sp}$ theoretically if $\eta$ and input power are the same, which means that plasma (chemical) propulsion has high (low) $I_{sp}$ but low (high) $F$.

#### 3.2.1. Single helicon thruster

There are many simple single helicon thrusters without any additional acceleration methods, and they have ElectroMagnets (EMs) and/or PMs. For compactness, in a relatively early phase of helicon experiments, sources with $D$ = 2–2.5 cm with $P_{rf}$

less than kW were attempted [96,97]. Note that decreasing the atomic mass from argon to helium and hydrogen showed a higher ion velocity up to 40 km/s owing to a lighter ion mass with external parameters not being changed appreciably [100]. Pulsed high-power helicon (HPH) thruster experiments to reach $n_e < 10^{14}$ cm$^{-3}$ with $P_{rf} > 10$ kW, focusing on magnetic nozzle effects, were executed using antenna 7 cm in diameter [186]. The nozzle effects under the divergent magnetic field configuration were studied [187] with a special thrust stand, which can distinguish among $T_s$ (static electron pressure force), $T_w$ (axial momentum loss delivered by ions to the radial wall), and $T_B$ (Lorentz force onto the magnetic nozzle). Here, $T_B$ is expressed by integrating in space the product of the electron diamagnetic current $j_\theta$ (azimuthal component) and the radial component of the external magnetic field $B_r$, and the measured $T_B$ was consistent with the theory [187].

Concerning compact PMs only experiments, plasmas with $D = 4.5$ cm [188] and 6.6 cm [189] showed a presence of ion beams of up to several tens of eV, relating to a double layer (DL) formation [184,190]. Here, DL is also called as an electrical double layer (EDL) that generally appears, e.g. on the surface of an object exposed in a fluid. In this layer in a plasma, a sharp potential drop greater than a few multiples of $T_e$ (strong electric field inside DL) and the violation of quasi-neutrality in both space charge layers occur. Here, DL with an ion-beam formation was found in the presence of a divergent magnetic field under a lower pressure range [191–194], e.g. < 0.1 Pa, the discharges of which do not imply the helicon plasma mode (but current-free DL character is found using a helicon source). Interesting phenomena were found on DL, e.g. three different populations of electron energy distribution functions downstream of DL [195], and potential drop was discussed with a presheath condition [196]. However, this use of DL formation with ion acceleration, so-called the Helicon Double Layer Thruster (HDLT), was not considered as another promising helicon thruster scheme afterwards, because the net momentum delivered by the large electric field in this DL is zero [197]. Note that DL is also considered to be important in space [191], e.g. in solar flares, a lunar wake behind the moon, and accelerated auroral particles, although these current driven systems are different from helicons of non-current driven systems.

A helicon source with larger size and higher $P_{rf}$ ranging from 0.2 to 200 kW showed better plasma performance, as shown in Figure 5 [198] from many machine data. This figure shows a tendency that the ratio of thrust $F$ to power, $F/P_{rf}$, increases with $P_{rf}$ but seems to saturate above 10 kW. However, this saturation level of 50 mN/kW is sufficient to compete with the Hall thruster case, where this thruster is widely used owing to its excellent thrust performance, but it does not have an electrodeless condition, as mentioned previously. As an example of the helicon thrust performance, in the range of $P_{rf} < 3$ kW, $F/P_{rf}$ and $I_{sp}$ were 21 (40) mN and 8.3 (16) mN/kW for argon (xenon) plasma, respectively [196]. The size effect can be also found with $D = 2.6$ and 9.5 cm [199]. In the latter diameter case, $F$ was ~ 18 (60) mN for $P_{rf}$ ~ 1 (6) kW.

### 3.2.2. Helicon thruster with additional acceleration scheme

Next, we describe additional acceleration schemes using helicon sources. In general, the control of thrust performance, such as $F$, $P_{rf}$, and $I_{sp}$, can be more flexible, although the overall thrust system becomes complex. Apart from VASIMR mentioned previously, experiments with an rf power level of typically a few kW have been performed as follows. Under the Helicon Electrodeless Advanced Thruster (HEAT) project, many acceleration methods are being tested [39,122]. Basically, electromagnetic acceleration by the axial Lorentz force with the product of the induced azimuthal electron current $j_\theta$ and external magnetic field $B_r$, has been investigated. This $j_\theta$ can be induced by (i) the rotating magnetic field (RMF) scheme [39, 122,200-203], the idea of which originates from the current drive method in FRC [204], (ii) the rotating electric field (REF) scheme [39,122,200,205], and (iii) a half cycle acceleration scheme with $m = 0$, low-frequency antenna current [39,42,122,200]. In order to induce a higher $j_\theta$, RMF (REF) penetration into a plasma is crucial [206] ([207]), in addition to $j_\theta$ penetration by the $m = 0$ scheme [39,122]. The other idea is ponderomotive acceleration combined with ICRH (so-called slow-wave heating similar to the acceleration scheme in VASIMR mentioned previously), e.g. [39,122,208]. Here, PA gives rise to the pure parallel acceleration of ions due to a localized electric field near the Ion Cyclotron Resonance (ICR) layer. On the other hand, the ICRH scheme causes perpendicular ion heating followed by energy conversion from the perpendicular to the parallel direction under a divergent magnetic field due to the conservation of magnetic moment. In this scheme, electromagnetic-field penetration into a plasma is also important [209].

Gridded helicon ion thrusters were investigated, although the electrodeless condition is not satisfied in the acceleration process and an additional neutralizer is necessary. The gridded helicon ion thruster (GHIT) [210], with screen and accelerator grids, was investigated in the case of $D = 14$ cm by measuring the ion beam current. It was found that the estimated cost of $E_i$ was 132–212 eV/ion with $P_{rf} < 600$ W and $B < 250$ G (EMs). The helicon electrostatic thruster (HEST) [211] in the case of $D = 2.7$ cm showed $I_{sp} \sim 2000$ s and $\eta$ of 9.7% with $P_{rf} < 1.5$ kW and $B$ up to 1 kG (combination of EMs and PMs). Here, a ring-shaped biased electrode, with 2.7-cm I.D. and 8-cm outer diameter, is located at the entrance of an expanded tube, and the ion beam energy increased almost linearly with the discharge voltage.

### 3.2.3. Various thrusters utilizing helicon sources

Here, we show various thrusters utilizing helicon sources, which have an advantage of highly efficient rf plasma production in an electrodeless condition, as mentioned previously.

A Mini-Magnetospheric Plasma Propulsion (M2P2) [212] scheme was proposed. A large-scale magnetic bubble around the spacecraft, i.e. an inflation of the dipole magnetic field produced by a high-density HP, is expected to allow the

spacecraft to ride solar wind to be accelerated. Here, a high efficiency was expected owing to the utilization of ambient energy of the solar wind.

Annularly bounded helicon waves [213] are analyzed to make a coaxial helicon source. This can be applied to a plasma source for a Hall thruster. With the same concept, the Helicon Hall thruster (HHT), an addition of a helicon source to a Hall thruster, is developed as a two-stage thruster to investigate an rf ionization stage (HP), which can improve the overall efficiency of a Hall thruster [214]. By combining helicon and MPD plasma sources, $n_e$ above $10^{14}$ cm$^{-3}$ with supersonic plasma flow (Mach number, which is the ion velocity normalized by the ion sound velocity, of ~1.8) was obtained, showing a higher thrust efficiency compared to the simple MPD thruster [215].

Note that helicon sources can be applied to a pre-ionization source in the thurster, e.g. Faraday Acceleration with Radio-Frequency Assisted Discharge (FARAD) [216]. There is a possibility that helicon sources can be utilized for air-breathing (i.e. collecting atmospheric gas for use as propellant) electric propulsion [217], compensating for drag on-orbit in Low Earth Orbit (LEO), instead of the objectives of, e.g. deep-space exploration and attitude control, as mentioned previously. Just recently, a review paper on space micropropulsion systems for CubeSats and small satellite, including small helicon sources, has been published [218]. Finally, at the end of this Section 3.2 on helicon thrusters, it must be noted that a biennial International Electric Propulsion Conference (IEPC) is being held, focusing on this emerging topic of plasma-based thrusters, including increased interest and research on helicon propulsion.

### 3.3. Industrial applications

In everyday life, many objects using mostly low-temperature plasmas can be observed [12,219–222], e.g. semiconductors fabricated using processes of deposition and etching, laser gases in discharges, and sterilization in medicine. Here, some typical practical applications of helicon sources are described, although we cannot cover all of them. Note that the understanding of plasma chemistry combined with plasma physics is also important, since many species of gases, including molecular, reactive gases in addition to noble gases, are used for various applications.

Ideal sources for industrial processing in a vacuum condition must have the following general characteristics: (i) simple, robust, and compact structure; (ii) large-area plasma uniformity; (iii) high-efficiency and high-speed processing including a high density with a low pressure; (iv) particle energy and orbit control; (v) good selectivity etc. In other words, flexibility to operate under a wide range of conditions is necessary for a good plasma source, depending on objectives.

In the processing of rf plasmas, compared to HP, CCP, and ICP are usually operated at lower electron densities with high pressures in order to obtain higher etch rates. Here, high-density sources such as HP are useful to reduce ion bombarding

damage due to a reduced sheath drop. Furthermore, there is another advantage that ion energy and angular spreads due to the collisionless condition become smaller. However, helicon sources have not been utilized widely for semiconductor fabrication, in spite of the merits of, e.g. shorter processing time due to the high density [abovementioned conditions (i)–(iv) can be easily satisfied]; instead, CCP and ICP sources are mostly being used.

In early phases, with helicon sources, the etch selectivity of Si and $SiO_2$ was examined using $SF_6$ gas [223,224]. These etch rates and their characteristics were investigated by fluorocarbon or chlorine gases [225,226]. In the case of the polysilicon etching, the *in situ* characterization of particle contamination showed few particles deposited onto the wafer [227], and both helicon and ECR sources showed a similar performance for the etching of polysilicon films using HBr gas with an addition of 3% $O_2$ gas [228]. Discharge characterization using $O_2$ gas was also performed [229,230]. Another example of using HP is the MØRI$^{TM}$ source with $D = 10$ cm and two antenna loops [231], which showed highly uniform plasmas and neutral distributions at the wafer location (process position), including, e.g. chlorine-based etch plasma. In addition, aluminum and tungsten interconnect etch, integrated poly-silicon etch, and oxide etch were tested. The fabrication of optical fibers was also investigated [232].

Further recent examples are as follows. A compact nitrogen radical source, useful for the fabrication of various nitride films, was developed [233], and antimony (Sb) films for optical recording were prepared [234]. Nanocrystalline (nc) $TiO_2$ films [235], which are outstanding as coating materials, and nc-SiC films, which are promising for use as short-wavelength light emitters, have been deposited [236]. In addition, nanostructure formation on tungsten targets was explored as a function of $He^+$ impact energy [237], the understanding of which is also important for developing the divertor in a tokamak [167] reactor.

## 4. Conclusions and future works

In this paper, we have discussed interesting HW plasma behaviors from various aspects. First, the basic features of HW were described in Section 2.1, which discussed two spatial modes of HW with a long radial wavelength and TG waves with a short wavelength, followed by a discussion of a highly efficient high-density plasma production mechanism in Section 2.2. Then, various helicon sources with the advantages of a very wide range of machine parameters, such as diameter, axial length, and the magnetic field in a cylindrical plasma, along with the effect of external operational parameters, were described in Section 2.3. In Section 3, the versatility of helicons for various applications was demonstrated. We have described applications to fundamental studies, which are very important for physical understandings based on useful helicon sources, including a torus geometry as well as a cylindrical one, chosen depending on objectives (Section 3.1). A special application example is a helicon thruster with a concept of the electrodeless

condition, leading to longer lifetime (Section 3.2). Finally, industrial applications, which have not been utilized thus far but need to be explored further in the future, were introduced with some examples (Section 3.3).

The following objectives need to be met in helicon science to be advanced in the future. Note that solving and comparing the differences between observations and theory are crucial for the advancement.

(i) A deeper and more detailed understanding of HW and TG wave phenomena is required, which would lead to high-density production with the use of more sophisticated diagnostics (and finer spatial resolutions to detect a short-wavelength TG wave pattern) utilizing, e.g. lasers and a new physical model. Numerical codes of FDTD, TASK/WF, particle in cell (PIC) [238], etc. will also be helpful. In addition, considering an electrostatic effect as well as an electromagnetic effect is necessary to have a full understanding of wave and plasma structures. A real antenna geometry with non-uniform plasma distributions in three dimensions is crucial for calculation. These will finally lead to the simulation of time evolution of plasma behaviors to conduct a comparative study with experimental results. Here, the non-linear coupling between the large amplitude excited wave and a plasma with non-uniform profiles must be understood self-consistently with spatio-temporal structures. However, there are many remaining problems, such anomalous ion heating [89] and excitation of high radial mode number of HW [21–23,25,115].

(ii) Further extension of the helicon source machine and plasma parameters is important. For example, machine geometries, machine sizes, magnetic field strength and its configuration, and working pressure must be improved. Further, an excitation frequency lower than a few hundred kHz (close to $f_{ci}$) or higher than GHz (close to $f_{ce}$) ranges, which depends on external parameters such as pressure and magnetic field, must be achieved, in addition to $n_e$ values well above $10^{14}$ cm$^{-3}$, for which the strong plasma-wall interaction and neutral density depletion must be considered. Concerning geometries, for example, it is very useful to produce high-density helicon plasma in a toroidal machine with a dipole field, Ring Trap-1 (RT-1) [239], aiming at high-beta, stable confinement for non-neutral plasmas. There is a possibility in a special magnetic field configuration using neutral line discharge (NLD) [240] that HW is excited to have an important role for plasma production. The operating neutral pressure $P_0$ is typically in the range of 0.1 to 1 Pa ($\nu/\omega$ up to ~7 was achieved [38]) but can theoretically be extended further, e.g. with increasing $B$ and $\omega$. As was mentioned previously, new applications to nuclear fusion machines are also promising, such as a current drive [177,178], which is suitable for off-axis driving [241], and high particle/heat fluxes [175,176] for irradiation of plasma-facing materials.

(iii) The advanced investigation of fundamental phenomena using the helicon sources mentioned in Section 3.1 is also crucial. Application to the following fields in laboratory and space is interesting to broaden the operational regions such as size, $n_e$, and $B_0$. This contributes to wider understandings of, e.g. magnetic reconnection in laboratory and space plasmas [19,242], dusty plasma [243], which is ubiquitous in the laboratory as well as plasma processing with low $n_e$ and low electron temperature, in addition to planetary rings and interstellar space. It is also interesting to investigate wave–particle interaction with propagating whistler mode waves in an auroral region, e.g. [244], as well as whistler soliton, e.g. [245], and lower hybrid solitary structures (sometimes called lower hybrid cavities) [246], which exhibit localized structures in space plasmas. We can perform simulation experiments on communication blackout [247], that is an important issue during the re-entry flight in an ionized plasma layer. Additionally, combined (or hybrid) operation, such as laser and HW, can widen the general research fields through the synergy effect.

(iv) Advanced thruster research and further extension to various practical applications are encouraging. Concerning thrusters, a more practical utilization from the near Earth, such as attitude control and a small satellite, to deep space in a human or non-human space flight can be expected, depending on objectives. Regarding industrial applications, R&D on environmental and medical fields can be expected, in addition to the present processes of plasma etching, deposition, spraying, and surface treatment for materials. Since the environment issue [248] is complex but of great concern, the overall understanding and mitigation of adverse effects are crucial. The emerging field of plasma medicine [249] is expected to play an important role in the near future, although it is still under development.

Finally, it can be stressed again that we expect the explosive evolution of featured, high-density helicon plasma sources, which have many advantages compared to other sources from the viewpoints of easy handling of high-density plasmas over a wide range of external parameters. Various ideas developed thus, far should be converted into practical devices for future innovative technologies in diverse fields as well as for contribution to basic fields for further development [220,221,248–250], as summarized again in Figure 8.

As was mentioned in the introduction, advances in plasma science have revealed many application fields such as energy, nanotechnology/materials, information/telecommunication, environment, space, biotechnology, etc. (bottom of Figure 8), considering seeds and needs. This also holds true for helicon plasma science, since helicon sources have been utilized in fields such basic plasma, plasma application, nuclear fusion, gas laser, plasma accelerator/thruster, and modelling in

space plasma, which were mentioned in Sections 2 and 3 (and the right-middle part of Figure 8).

Note that it is necessary to understand and control the non-linearity of plasma with a complex structural formation for the evolution of extensive plasma science. New concepts, new regions of various parameters (development and its application: left-middle part of Figure 8), and new methods can advance plasma science (top-right part of Figure 8) to achieve the new understandings and identify new applications.

## Acknowledgement

The author would like to thank many researchers around the world for fruitful discussions. Furthermore, the author is grateful for significant contributions made by many past collaborators, especially late Prof. K. Toki and late Dr K. P. Shamrai. Our LHPD experiments were conducted in and supported by the Space Plasma Laboratory at ISAS, JAXA under their research collaboration program.

## Disclosure statement

The author declares no potential conflict of interest.

## Funding

This work was partly supported by the Grant-in-Aid for Scientific Research under Grant S: 21226019 through the Japan Society for the Promotion of Science.

## References

[1] R.W. Boswell, Phys. Lett. 33A (1970) p.457.
[2] S. Shinohara, Jpn. J. Appl. Phys. 36 (1997) p.4695 (review paper), and references therein.
[3] R.W. Boswell and F.F. Chen, IEEE Trans. Plasma Sci. 25 (1997) p.1229 (review paper), and references therein.
[4] F.F. Chen and R.W. Boswell, IEEE Trans. Plasma Sci. 25 (1997) p.1245 (review paper), and references therein.
[5] S. Shinohara, J. Plasma Fusion Res. 78 (2002) p.5 (review paper), and references therein [in Japanese].
[6] S. Shinohara, Butsuri 64 (2009) p.519 (review paper), and references therein [in Japanese].
[7] F.F. Chen, Plasma Sources Sci. Technol. 24 (2015) p.014001 (review paper), and references therein.
[8] E.E. Scime, A.M. Keesee and R.W. Boswell, Phys. Plasmas 15 (2008) p.058301 (mini-conference), and references therein.
[9] J.A. Lehane and P.C. Thonemann, Proc. Phys. Soc. 85 (1965) p.301.
[10] D.G. Swanson, *Plasma Waves*, Academic Press, San Diego, CA, 1989.
[11] T.H. Stix, *Waves in Plasmas*, American Institute of Physics, New York, NY, 1992.
[12] M.A. Lieberman and A.J. Lichtenberg, *Principals of Plasma Discharges and Materials Processing*, Wiley, New York, 1994.
[13] R.L. Stenzel, Adv. Phys.: X 1 (2015) p.687 (review paper), and references therein.

[14] J. Hopwood, Plasma Sources Sci. Technol. 1 (1992) p.109 (review paper), and references therein.
[15] V. Godyak, Plasma Phys. Control. Fusion. 1 (2003) p.A339 (review paper), and references therein.
[16] F.F. Chen, Plasma Phys. Control. Fusion 33 (1991) p.339.
[17] H.A.B. Bodin, Nucl. Fusion 30 (1991) p.1717 (review paper), and references therein.
[18] J.B. Taylor, Phys. Rev. Lett. 33 (1974) p.1139.
[19] M.A. Berger, Plasma Phys. Control. Fusion 41 (1999) p.B167 (review paper), and references therein.
[20] S.M. Mahajan and Z. Yoshida, Phys. Rev. Lett. 81 (1998) p.4863.
[21] Y. Sakawa, N. Koshikawa and T. Shoji, Plasma Sources Sci. Technol. 8 (1997) p.96.
[22] M. Light, I.D. Sudit, F.F. Chen and D. Arnush, Phys. Plasmas 2 (1998) p.4094.
[23] H. Takeno, Y. Yasaka, O. Sakai and R. Itatani, Nucl. Fusion 35 (1999) p.75.
[24] T. Motomura, S. Shinohara, T. Tanikawa and K.P. Shamrai, Phys. Plasmas 81 (2012) p.043504.
[25] B.P. Cluggish, F.A. Anderegg, R.L. Freeman, J. Gilleland, T.J. Hilsabeck, P.C. Isler, W.D. Lee, A.A. Litvak, R.L. Miller, T. Ohkawa, S. Putvinski, K.R. Umstadter and D.L. Winslow, Phys. Plasmas 12 (2005) p.057101.
[26] M. Nisoa, Y. Sakawa and T. Shoji, Jpn. J. Apply. Phys. 38 (1999) p.L777.
[27] S. Shinohara, T. Hada, T. Motomura, K. Tanaka, T. Tanikawa, K. Toki, Y. Tanaka and K.P. Shamrai, Phys. Plasmas 16 (2009) p.057104.
[28] T. Watari, T. Hatori, R. Kumazawa, S. Hidekuma, T. Aoki, T. Kawamoto, M. Inutake, S. Hiroe, A. Nishizawa, K. Adati, T. Sato, T. Watanabe, H. Obayashi and K. Takayama, Phys. Fluids 21 (1978) p.2076.
[29] J.E. Stevens, M.J. Sowa and J.L. Cecchi, J. Vac. Sci. Technol. A13 (1995) p.2476.
[30] S. Shinohara, S. Takechi and Y. Kawai, Jpn. J. Appl. Phys. 35 (1996) p.4503.
[31] Y. Yasaka and Y. Hara, Jpn. J. Appl. Phys. 33 (1994) p.5950.
[32] S. Shinohara, Y. Miyauchi and Y. Kawai, Plasma Phys. Control. Fusion 37 (1995) p.1015.
[33] R.L. Stenzel and J.M. Urrutia, Phys. Rev. Lett. 114 (2015) p.205005.
[34] J.-H. Kim, S.-M. Yun and H.-Y. Chang, IEEE Trans. Plasma Sci. 24 (1996) p.1364.
[35] M. Krämer, B. Lorenz and B. Clarenbach, Plasma Sources Sci. Technol. 11 (2002) p.A120.
[36] S. Shinohara, T. Tanikawa and T. Motomura, Rev. Sci. Instrum. 85 (2014) p.093509.
[37] S. Shinohara, N. Kaneda and Y. Kawai, Thin Solid Films. 316 (1998) p.139.
[38] S. Shinohara and K. Yonekura, Plasma Phys. Control. Fusion 42 (2000) p.41.
[39] S. Shinohara, H. Nishida, T. Tanikawa, T. Hada, I. Funaki and K.P. Shamrai, IEEE Trans. Plasma Sci. 42 (2014) p.1245.
[40] S. Shinohara and T. Tanikawa, Rev. Sci. Instrum. 75 (2004) p.1941.
[41] S. Shinohara and T. Tanikawa, Phys. Plasmas 12 (2005) p.044502.
[42] T. Ishii, H. Ishii, S. Otsuka, N. Teshigahara, H. Fujitsuka, S. Waseda, D. Kuwahara, and S. Shinohara, JPS Conf. Proc 1 (2014) p. 015047.
[43] T. Tanikawa and S. Shinohara, in *Proc. Int. Cong. Plasma Phys.*, Nice, 2004.
[44] S. Shinohara, D. Kuwahara, T. Ishii, H. Iwaya, S. Nishimura, T. Yamase, D. Arai and H. Horita, IEEE Trans. Plasma Sci. 46 (in press).
[45] J. Vlček, J. Phys. D: Appl. Phys. 22 (1989) p.623.
[46] S. Waseda, H. Fujitsuka, S. Shinohara, D. Kuwahara, M. Sakata and H. Akatsuka, Plasma Fusion Res. 9 (2014) p.340612.
[47] K.P. Shamrai and K.R. Taranov, Plasma Sources Sci. Technol. 5 (1996) p.474.
[48] A.I. Akhiezer, V.S. Mikhailenko and K.N. Stepanov, Phys. Lett. A 245 (1998) p.117.
[49] V.F. Virko, G.S. Kirichenko and K.P. Shamrai, Plasma Sources Sci. Technol. 12 (2003) p.203.

[50] B. Lorenz, M. Krämer, V.L. Selenin and Y.M. Aliev, Plasma Sources Sci. Technol. 14 (2005) p.623.
[51] B.N. Breizman and A.V. Arefiev, Phys. Rev. Lett. 84 (2000) p.3863.
[52] P.K. Loewenhardt, B.D. Blackwell, R.W. Boswell, G.D. Conway and S.M. Hamberger, Phys. Rev. Lett. 67 (1991) p.2792.
[53] F.F. Chen and D.D. Blackwell, Phys. Rev. Lett. 82 (1999) p.2677.
[54] S. Cho, Phys. Plasmas 3 (1996) p.4268.
[55] I.V. Kamenski and G.G. Borg, Phys. Plasmas 3 (1996) p.4396.
[56] Y. Mouzouris and J. Scharer, IEEE Trans. Plasma Sci. 24 (1996) p.152.
[57] X.M. Guo, J. Scharer, Y. Mouzouris and L. Louis, Phys. Plasmas 6 (1999) p.3400.
[58] D. Arnush and F.F. Chen, Phys. Plasmas 4 (1997) p.3411.
[59] D. Arnush and F.F. Chen, Phys. Plasmas 5 (1998) p.1239.
[60] D. Arnush, Phys. Plasmas 7 (2000) p.3042.
[61] www.seas.ucla.edu/ltptl/presentations.htm (HELIC 10zip.exe).
[62] D. Melazzi, D. Curreli, M. Manente, J. Carlsson and D. Pavarin, Comp. Phys. Commun. 183 (2012) p.1182.
[63] D. Melazzi and V. Lancellotti, Comp. Phys. Commun. 185 (2014) p.1914.
[64] J. Jacquinot, B.D. McVey and J.E. Scharer, Phys. Rev. Lett. 39 (1977) p.1577.
[65] K. Ida, O. Naito, I. Ochiai, S. Shinohara and K. Miyamoto, Nucl. Fusion 24 (1984) p.375.
[66] S. Shinohara and K.P. Shamrai, Plasma Phys. Control. Fusion 42 (2000) p.865.
[67] K.P. Shamrai and S. Shinohara, Phys. Plasmas 8 (2001) p.4659.
[68] T. Lho, N. Hershkowitz, J. Miller, W. Steer and G.H. Kim, Phys. Plasmas 5 (1998) p.3135.
[69] D.D. Blackwell, T.G. Madziwa, D. Arnush and F.F. Chen, Phys. Rev. Lett. 88 (2002) p.145002.
[70] S. Isayama, T. Hada and S. Shinohara, Phys. Plasmas 23 (2016) p.063513.
[71] S. Shinohara and Y. Kawai, Jpn. J. Appl. Phys. 34 (1995) p.L1571.
[72] S. Shinohara, Y. Miyauchi and Y. Kawai, Jpn. J. Appl. Phys. 35 (1996) p.L731.
[73] R.W. Boswell, Plasma Phys. Control. Fusion 26 (1984) p.1147.
[74] J. Scharer, A. Degeling, G. Borg and R.W. Boswell, Phys. Plasmas 9 (2002) p.3734.
[75] S. Shinohara and T. Tanikawa, Thin Solid Films. 506–507 (2006) p.559.
[76] S. Shinohara, S. Takechi, N. Kaneda and Y. Kawai, Plasma Phys. Control. Fusion 39 (1997) p.1479.
[77] S. Shinohara and T. Soejima, Plasma Phys. Control. Fusion 40 (1998) p.2081.
[78] S. Shinohara and K.P. Shamrai, Thin Solid Films 407 (2002) p.215.
[79] S. Shinohara and K.P. Shamrai, Thin Solid Films 506–507 (2006) p.555.
[80] C. Watts, Rev. Sci. Instrum. 75 (2004) p.1975.
[81] A.G. Lynn, M. Gilmore, C. Watts, J. Herrea, R. Kelly, S. Will, S. Xie, L. Yan and Y. Zhang, Rev. Sci. Instrum. 80 (2009) p.103501.
[82] F.F. Chen and H. Torreblanca, Phys. Plasmas 16 (2009) p.057102.
[83] C.M. Franck, O. Grulke and T. Klinger, Phys. Plasmas 9 (2002) p.3254.
[84] C.M. Franck, O. Grulke and T. Klinger, Phys. Plasmas 10 (2003) p.323.
[85] G.R. Tynan, M.J. Burin, C. Holland, G. Antar, N. Crocker and P.H. Diamond, Phys. Plasmas 11 (2004) p.5195.
[86] C. Holland, J.H. Yu, A. James, D. Nishijima, M. Shimada, N. Taheri and G.R. Tynan, Phys. Rev. Lett. 96 (2006) p.195002.
[87] J. Hana and C. Watts, Phys. Plasmas 8 (2001) p.4251.
[88] P.A. Keiter, E.E. Scime and M. Balkey, Phys. Plasmas 4 (1997) p.2741.
[89] M.W. Balkey, R. Boivin, J.L. Kline and E.E. Scime, Plasma Sources Sci. Technol. 10 (2001) p.284.

[90] Å. Fredriksen, L.N. Mishra, N. Gulbrandsen and W.J. Miloch, J. Phys.: Conf. Ser. 257 (2010) p.012019.
[91] R.D. Brown, J.H. Gilland, N. Hershkowitz and R.A. Breun, J. Vac. Sci. Technol. A13 (1995) p.865.
[92] S.M. Tysk, C.M. Denning, J.E. Scharer and K. Akhtar, Phys. Plasmas 11 (2004) p.878.
[93] F.F. Chen, J. Vac. Sci. Technol. A10 (1992) p.1389.
[94] T. Shoji, Y. Sakawa, S. Nakazawa, K. Kadota and T. Sato, Plasma Sources Sci. Technol. 2 (1993) p.5.
[95] Y. Sakawa, H. Kunimatsu, H. Kikuchi, Y. Fukui and T. Shoji, Phys. Rev. Lett. 90 (2003) p.105001.
[96] K. Toki, S. Shinohara, T. Tanikawa and K.P. Shamrai, 506–507 (2006) p.597.
[97] O.V. Batishchev, IEEE Trans. Plasma Sci. 37 (2009) p.1563.
[98] D. Kuwahara, A. Mishio, T. Nakagawa and S. Shinohara, Rev. Sci. Instrum. 84 (2013) p.103502.
[99] T. Nakagawa, S. Shinohara, D. Kuwahara, A. Mishio, H. Fujitsuka and J.P.S. Conf, Proc. 1 (2014) p.015002.
[100] T. Nakagawa, Y. Sato, H. Iwaya, D. Kuwahara and S. Shinohara, Plasma Fusion Res. 10 (2015) p.3401037.
[101] S. Shinohara and H. Mizokoshi, Rev Sci. Instrum. 77 (2006) p.036108.
[102] F.R. Chang-Díaz, Sci. Am. 283 (2000) p.90.
[103] B.W. Longmier, J.P. Squire, M.D. Carter, L.D. Cassady, T.W. Glover, W.J. Chancery, C.S. Olsen, A.V. Ilin, G.E. McCaskill, and F.R. Chang-Díaz, in *Proc. 45th AIAA/ASME/SAE/ASEE Joint Propulsion Conference & Exhibit*, Denver, CO, 2009, AIAA, p.2009–5359.
[104] https://en.wikipedia.org/wiki/Variable_Specific_Impulse_Magnetoplasma_Rocket.
[105] K.P. Shamrai, V.F. Virko, H.-O. Blom, V.P. Pavlenko, V.B. Taranov, L.B. Jonsson, C. Hedlund and S. Berg, J. Vac. Sci. Technol. A15 (1997) p.2864.
[106] K.P. Shamrai, Plasma Sources Sci. Technol. 7 (1998) p.499.
[107] K. Takahashi, D. Sato, K. Takaki and A. Ando, Plasma Sources Sci. Technol. 22 (2013) p.055002.
[108] F.F. Chen, X. Jiang, J.D. Evans, G. Tynan and D. Arnush, Plasma Phys. Control. Fusion 39 (1997) p.A411.
[109] F.F. Chen, Phys. Plasmas 10 (2003) p.2586.
[110] A.W. Degeling, G.G. Borg and R.W. Boswell, Phys. Plasmas 11 (2004) p.2144.
[111] T. Lafleur, C. Charles and R.W. Boswell, Phys. Plasmas 17 (2010) p.073508.
[112] S. Takechi and S. Shinohara, Jpn. J. Appl. Phys. 38 (1999) p.L1278.
[113] F.F. Chen, J. Vac. Sci. Techonol. A10 (1992) p.1389.
[114] K.P. Shamrai, S. Shinohara, V.F. Virko, V.M. Slobodyan, YuV Virko and G.S. Kirichenko, Plasma Phys. Control. Fusion 47 (2005) p.A307.
[115] S. Takechi, S. Shinohara and Y. Kawai, Jpn. J. Appl. Phys. 36 (1997) p.4558.
[116] S. Takechi, S. Shinohara and Y. Kawai, Surf. Coat. Technol. 112 (1999) p.15.
[117] S. Takechi, S. Shinohara and A. Fukuyama, Jpn. J. Appl. Phys. 38 (1999) p.3716.
[118] K. Takahashi, S. Takayama, A. Komoro and A. Ando, Phys. Rev. Lett. 116 (2016) p.135001.
[119] G.S. Eom, I.D. Bae, G. Cho, Y.S. Hwang and W. Choe, Plasma Sources Sci. Technol. 10 (2001) p.417.
[120] H. Kikuchi, Y. Fukui, Y. Sakawa and T. Shoji, Phys. Plasmas 10 (2003) p.521.
[121] Y. Sakawa, H. Kunimatsu, H. Kikuchi, Y. Fukui and T. Shoji, Phys. Rev. Lett. 90 (2003) p.105001.
[122] S. Shinohara, J. Plasma Fusion Res. 91 (2015) p.412 (project review paper), and references therein. [in Japanese].

[123] P. Zhu and R.W. Boswell, Phys. Rev. Lett. 63 (1989) p.2805.
[124] S. Yun, J. Kim and H. Chang, J. Vac. Sci. Technol. A15 (1997) p.673.
[125] Y. Sakawa, T. Takino and T. Shoji, Phys. Plasmas 6 (1999) p.4759.
[126] S. Cho, Phys. Plasmas 6 (1999) p.359.
[127] M. Porkolab, J.J. Schuss, B. Lloyd, Y. Takase, S. Texter, P. Bonoli, C. Fiore, R. Gandy, D. Gwinn, B. Lipschultz, E. Marmar, D. Pappas, R. Parker and P. Pribyl, Phys. Rev. Lett. 53 (1984) p.450.
[128] J. Gilland, R. Breun and N. Hershkowitz, Plasma Sources Sci. Technol. 7 (1998) p.416.
[129] S. Yun, K. Taylor and G. Tynan, Phys. Plasmas 7 (2000) p.3448.
[130] B. Clarenbach, B. Lorenz, M. Krämer and N. Sadeghi, Plasma Sources Sci. Technol. 12 (2003) p.345.
[131] A.M. Keesee and E.E. Scime, Plasma Sources Sci. Technol. 16 (2007) p.742.
[132] M.E. Galante, R.M. Magee and E.E. Scime, Phys. Plasmas 21 (2014) p.055704.
[133] A. Fruchtman, J. Phys. D: Applied Phys. 50 (2017) p.473002 (review paper), and references therein.
[134] S. Shinohara, D. Kuwahara, K. Yano and A. Fruchtman, Phys. Plasmas 23 (2016) p.122108.
[135] A. Fruchtman and S. Shinohara, Phys. Plasmas 24 (2017) p.103523.
[136] M. Ignatenko, M. Azumi, M. Yagi, S. Shinohara, S.-I. Itoh and K. Itoh, Jpn. J. Appl. Phys. 46 (2007) p.1680.
[137] Y. Saitou, A. Yonesu, S. Shinohara, M.V. Ignatenko, N. Kasuya, M. Kawaguchi, K. Terasaka, T. Nishijima, Y. Nagashima, Y. Kawai, M. Yagi, S.-I. Itoh, M. Azumi and K. Itoh, Phys. Plasmas 14 (2007) p.072301.
[138] K. Takahashi, Y. Takao and A. Ando, Appl. Phys. Lett. 109 (2016) p.194101.
[139] S. Shinohara, N. Matsuoka and Y. Kawai, Jpn. J. Appl. Phys. 38 (1999) p.4321.
[140] S. Shinohara, H. Tsuji, T. Yoshinaka and Y. Kawai, Surf. Coat. Tehnol. 112 (1999) p.20.
[141] S. Shinohara, N. Matsuoka and S. Matsuyama, Phys. Plasmas 8 (2001) p.1154.
[142] S. Shinohara, N. Matsuoka and S. Matsuyama, Trans: Fusion Technol. 39 (2001) p.358.
[143] S. Matsuyama, S. Shinohara and O. Kaneko, Trans: Fusion Technol. 39 (2001) p.362.
[144] S. Shinohara, S. Matsuyama and O. Kaneko, Thin Solid Films 407 (2002) p.209.
[145] S. Matsuyama and S. Shinohara, J. Plasma Fusion Res. SERIES 4 (2001) p.528.
[146] F. Wagner, G. Fussmann, T. Grave, M. Keilhacker, M. Kornherr, K. Lackner, K. McCormick, E.R. Müller, A. Stäbler, G. Becker, K. Bernhardi, U. Ditte, A. Eberhagen, O. Gehre, J. Gernhardt, G.V. Gierke, E. Glock, O. Gruber, G. Haas, M. Hesse, G. Janeschitz, F. Karger, S. Kissel, O. Klüber, G. Lisitano, H.M. Mayer, D. Meisel, V. Mertens, H. Murmann, W. Poschenrieder, H. Rapp, H. Röhr, F. Ryter, F. Schneider, G. Siller, P. Smeulders, F. Söldner, E. Speth, K.-H. Steuer, Z. Szymanski and O. Vollmer, Phys. Rev. Lett. 53 (1984) p.1453.
[147] S. Shinohara and S. Matsuyama, Phys. Plasmas 9 (2002) p.4540.
[148] S. Shinohara, Y. Nakamura and S. Horii, Phys. Thin Solid Films 506–507 (2006) p.564.
[149] T. Ohkawa and R. Miller, Phys. Plasmas 9 (2002) p.5116.
[150] S. Shinohara and S. Horii, Jpn. J. Appl. Phys. 46 (2007) p.4276.
[151] R. Gueroult, E.S. Evans, S.J. Zweben, N.J. Fisch and F. Levinton, Plasma Sources Sci. Technol. 25 (2006) p.035204.
[152] S. Shinohara and A. Fujii, Phys. Plasmas 8 (2001) p.3018.
[153] A. Fukuyama and Y. Ichida, in *Proc. of the 1996 Int. Conf. on Plasma Phys., Nagoya, 1996*, H. Sugai and T. Hayashi, eds., The Japan Society of Plasma Science and Nuclear Fusion Research, Nagoya, 2, 1997, p.1342.
[154] C.M. Frank, O. Grulke and T. Klingeer, Phys. Plasmas 9 (2002) p.3524.
[155] M. Light, F.F. Chen and P.L. Colestock, Phys. Plasmas 8 (2001) p.4675.

[156] O. Grulke, F. Greiner, T. Klinger and A. Piel, Plasma Phys. Control. Fusion 43 (2003) p.525.
[157] C. Schröder, O. Grulke, T. Klinger and V. Naulin, Phys. Plasmas 11 (2004) p.4249.
[158] T. Yamada, S.-I. Itoh, T. Maruta, N. Kasuya, Y. Nagashima, S. Shinohara, K. Terasaka, M. Yagi, S. Inagaki, Y. Kawai, A. Fujisawa and K. Itoh, Nature Phys. 4 (2008) p.721.
[159] Y. Nagashima, S.-I. Itoh, S. Shinohara, M. Fukao, A. Fujisawa, K. Terasaka, Y. Kawai, G.R. Tynan, P.H. Diamond, M. Yagi, S. Inagaki, T. Yamada and K. Itoh, Phys. Plasmas 16 (2009) p.020706.
[160] H. Arakawa, K. Kamataki, S. Inagaki, T. Maruta, Y. Nagashima, T. Yamada, S. Shinohara, K. Terasaka, S. Sugita, M. Yagi, N. Kasuya, A. Fujisawa, S.-I. Itoh and K. Itoh, Plasma Phys. Control. Fusion 51 (2009) p.085001.
[161] T. Yamada, S.-I. Itoh, S. Inagaki, Y. Nagashima, S. Shinohara, N. Kasuya, K. Terasaka, K. Kamataki, H. Arakawa, M. Yagi, A. Fujisawa and K. Itoh, Phys. Plasmas 17 (2010) p.052313.
[162] P. Manz, M. Xu, S.C. Thakur and G.R. Tynan, Plasma Phys. Control. Fusion 53 (2011) p.095001.
[163] Y. Nagashima, S.-I. Itoh, S. Inagaki, H. Arakawa, N. Kauya, A. Fujisawa, K. Kamataki, T. Yamada, S. Shinohara, S. Oldenbürger, M. Yagi, Y. Takase, P.H. Diamond and K. Itoh, Phys. Plasmas 18 (2011) p.070701.
[164] S.C. Thakur, M. Xu, P. Manz, N. Fedorczak, C. Holland and G. R. Tynan, Phys. Plasmas 20 (2013) p.012304.
[165] N. Krause, C. Lechte, J. Stöber, U. Stroth, E. Ascasibar and J. Alonso, Rev. Sci. Instrum. 73 (2002) p.3474.
[166] T.R. Desjardins and M. Gilmore, Phys. Plasmas 23 (2016) p.055710.
[167] K. Miyamoto, *Plasma Physics and Controlled Nuclear Fusion*, Springer-Verlag, Berlin, 2005.
[168] E.E. Scime, P.A. Keiter, M.M. Balkey, R.F. Boivin, J.L. Kline and M. Blackburn, Phys. Plasmas 7 (2000) p.2157.
[169] C.S. Corr and R.W. Boswell, Phys. Plasmas 14 (2007) p.122503.
[170] S. Shinohara, T. Motomura, K. Tanaka, T. Tanikawa and K.P. Shamrai, Plasma Sources Sci. Technol. 19 (2010) p.034018.
[171] Y.S. Hwang, I.S. Hong and G.S. Eom, Rev. Sci. Instrum. 69 (1998) p.1344.
[172] O. Tarvainen, M. Light, G. Rouleau and R. Keller, AIP Conf. Proc. 925 (2007) p.171.
[173] H.D. Jung, M.J. Park, S.H. Kim and Y.S. Hwang, Rev. Sci. Instrum. 75 (2004) p.1878.
[174] R. Aymar, P. Barabasch and Y. Shimomura, Plasma Phys. Contol. Fusion 44 (2002) p.419.
[175] B.D. Blackwell, J.F. Caneses, C.M. Samuell, J. Wach, J. Howard and C. Corr, Plasma Sources Sci. Technol. 21 (2012) p.055033.
[176] J. Rapp, T.M. Biewer, T.S. Bigelow, J.B.O. Caughman, R.C. Duckworth, R.J. Ellis, D.R. Giuliano, R.H. Goulding, D.L. Hillis, R.H. Howard, T.L. Lessard, J.D. Lore, A. Lumsdaine, E.J. Martin, W.D. McGinnis, S.J. Meitner, L.W. Owen, H.B. Ray, G.C. Shaw and V.K. Varma, IEEE Trans. Plasma Sources Sci. 44 (2016) p.3456.
[177] O. Grulke, F. Greiner, T. Klinger and A. Piel, Plasma Phys. Control. Fusion 43 (2001) p.525.
[178] S.K. Tripathi and D. Bora, Nucl. Fusion 42 (2002) p.L15.
[179] Y. Sakawa, M. Oshima, Y. Ohta and T. Shoji, Phys. Plasmas 10 (2003) p.3447.
[180] M.G. Shats, D.L. Rudakov, R.W. Boswell and G.G. Borg, Phys. Plasmas 4 (1997) p.3629.
[181] A.C. Hossack, T. Firman, T.R. Jarboe, J.R. Prager, B.S. Victor, J.S. Wrobel and T. Ziemba, Rev. Sci. Instrum. 84 (2013) p.103506.
[182] R.G. Jahn, *Physics of Electric Propulsion*, Dover Publications, New York, 2006.

[183] C. Charles, J. Phys. D: Appl. Phys. 42 (2009) p.163001 (topical review paper), and references therein.
[184] B.W. Longmier, J.P. Squire, C.S. Olsen, L.D. Cassady, M.G. Ballenger, M.D. Carter, A.V. Ilin, T.W. Glover, G.E. McCaskill, F.R. Chang Díaz and J. Propul, Power 30 (2014) p.123.
[185] E.A. Bering III, F.R. Chang-Díaz, J.P. Squire, T.W. Glover, M.D. Carter, G.E. McCaskill, B.W. Longmier, M.S. Brukardt, W.J. Chancery and V.T. Jacobson, Phys. Plasmas 17 (2010) p.043509.
[186] R. Winglee, T. Ziemba, L. Giersch, J. Prager, J. Carscadden and B.R. Roberson, Phys. Plasmas 14 (2007) p.063501.
[187] K. Takahashi, T. Lafleur, C. Charles, P. Alexander and R.W. Boswell, Phys. Rev. Lett. 107 (2011) p.235001.
[188] YuV Virko, V.F. Virko, K.P. Shamrai and A.I. Yakimenko, Prob. Atomic Sci. Technol., No. 1 Series: Plasma Phys. 13 (2007) p.136.
[189] K. Takahashi, K. Oguni, H. Yamada and T. Fujiwara, Phys. Plasmas 15 (2008) p.084501.
[190] L.P. Block, Astrophys. Space Sci. 55 (1978) p.59 (review paper), and references therein.
[191] C. Charles, Plasma Sources Sci. Technol. 16 (2007) p.R1 (topical review paper), and references therein.
[192] S.A. Cohen, N.S. Siefert, S. Stange, R.F. Boivin, E.E. Scime and F.M. Levinton, Phys. Plasmas 10 (2003) p.2593.
[193] C. Charles and R.W. Boswell, Phys. Plasmas 11 (2004) p.1706.
[194] N. Plihon, P. Chabert and C.S. Corr, Phys. Plasmas 14 (2007) p.013506.
[195] K. Takahashi, C. Charles, R. Boswell, W. Cox and R. Hatakeyama, Appl. Phys. Lett. 94 (2009) p.191503.
[196] F.F. Chen, Phys. Plasmas 13 (2006) p.034502.
[197] A. Fruchtman, Phys. Rev. Lett. 96 (2006) p.065002.
[198] D. Kuwahara, S. Shinohara and K. Yano, J. Propul. Power 33 (2017) p.420.
[199] K. Takahashi, A. Komuro and A. Ando, Plasma Sources Sci. Technol. 24 (2015) p.055105.
[200] S. Shinohara, T. Tanikawa, T. Hada, I. Funaki, H. Nishida, T. Matsuoka, F. Otsuka, K.P. Shamrai, T.S. Rudenko, T. Nakamura, A. Mishio, H. Ishii, N. Teshigahara, H. Fujitsuoka and S. Waseda, Trans. Fusion Sci. Technol. 63 (2013) p.164.
[201] S. Otsuka, T. Nakagawa, H. Ishii, N. Teshigahara, H. Fujituska, S. Waseda, T. Ishii, D. Kuwahara and S. Shinohara, Plasma Fusion Resarch 9 (2014) p.3406047.
[202] T. Furukawa, K. Takizawa, D. Kuwahara and S. Shinohara, Phys. Plasmas 24 (2017) p.043505.
[203] T. Furukawa, K. Takizawa, D. Kuwahara and S. Shinohara, AIP Advances 7 (2017) p.115204.
[204] I.R. Jones, Phys. Plasmas 6 (1999) p.1950 (review paper), and references therein.
[205] T. Nakamura, K. Yokoi, H. Nishida, T. Matsuoka, I. Funaki, S. Shinohara, T. Tanikawa, T. Hada, T. Motomura, K.P. Shamrai and T.S. Rudenko, Trans. JSASS Aerospace Tech. Japan 10 (2012) p.Tb_17.
[206] R.D. Milroy, Phys. Plasmas 6 (1999) p.2771.
[207] T. Matsuoka, T.S. Rudenko, I. Funaki, K.P. Shamrai, T. Nakamura, H. Nishida, T. Tanikawa, T. Hada and S. Shinohara, Jpn. J. Appl. Phys. 51 (2012) p.096201.
[208] F. Otsuka, T. Hada, S. Shinohara, T. Tanikawa and T. Matsuoka, Plasma Fusion Res. 8 (2013) p.1406012.
[209] F. Otsuka, T. Hada, S. Shinohara and T. Tanikawa, Planets and Space 65 (2015) p.85.
[210] L.T. Williams and M.L.R. Walker, Plasma Sources Sci. Technol. 22 (2013) p.055019.
[211] A. Uchigashima, T. Baba, D. Ichihara, A. Iwakawa, A. Sasoh, T. Yamazaki, S. Harada, M. Sasahara and T. Iwasaki, IEEE Trans. Plasma. Sci. 44 (2016) p.306.
[212] R.M. Winglee, J. Slough, T. Ziemba and A. Goodson, J. Geophys. Res. 105 (2000) p.21067.

[213] M. Yano and M.L.R. Walker, Phys. Plasmas 13 (2006) p.063501.
[214] S. Shabshelowitz, A.D. Gallimore and Y.P.Y. Peterson, J. Propul. Power 30 (2014) p.664.
[215] K. Takahashi, A. Komuro and A. Ando, Apply: Phys. Lett. 105 (2014) p.193503.
[216] E.Y. Choueiri and K.A. Polzin, in *Proc. 40th AIAA/SAE/ASME/ASEE Joint Propulsion Conference*, Ft. Lauderdale, 2004, AIAA, p.2004–3940.
[217] L.A. Singh and M.L.R. Walker, Prog. Aerosp. Sci. 75 (2015) p.15 (review paper), and references therein.
[218] I. Levchenko, K. Bazaka, Y. Ding, Y. Raitses, S. Mazouffre, T. Henning, P.J. Klar, S. Shinohara, J. Schein, L. Garrigues, M. Kim, D. Lev, F. Taccogna, R.W. Boswell, C. Charles, H. Koizumi, S. Yan, C. Scharlemann, M. Keidar and X. Shuyan, Appl. Phys. Rev. 4 (in press).
[219] J. R. Roth, *Industrial Engineering: Volume 1: Principles*, Institute of Physics Publishing, Bristol, 1995.
[220] F.F. Chen, Phys. Plasmas 2 (1995) p.2164.
[221] Plasma 2010 Committee, Plasma Science Committee, Board on Physics and Astronomy, Division on Engineering and Physical Science and National Research Council of the National Academies, *Plasma Science: Advancing Knowledge in the National Interest*, The National Academic Press, Washington, DC, 2007.
[222] S. Samukawa, M. Hori, S. Rauf, K. Tachibana, P. Bruggeman, G. Kroesen, J.C. Whitehead, A.B. Murphy, A.F. Gutsol, S. Starikovskaia, U. Kortshagen, J.-P. Boeuf, T.J. Sommerer, M.J. Kushner, U. Czarnetzki and N. Mason, J. Phys. D: Appl. Phys. 45 (2012) p.253001 (review paper), and references therein.
[223] R.W. Boswell and D. Henry, Appl. Phys. Lett. 47 (1985) p.1095.
[224] R.W. Boswell and R.K. Porteus, J. Appl. Phys. 62 (1987) p.3123.
[225] H. Kitagawa, A. Tsunoda, H. Shindo and Y. Horiike, Plasma Sources Sci. Technol. 2 (1993) p.11.
[226] T. Tsukada, H. Nogami, Y. Nakagawa and E. Wani, Jpn. J. Appl. Phys. 33 (1994) p.4433.
[227] G.S. Selwyn and A.D. Bailey, J. Vac. Sci. Technol. A 14 (1996) p.649.
[228] I. Tepermeister, D.E. Ibbotson, J.T.C. Lee and H.H. Sawin, J. Vac. Sci. Technol. B 12 (1994) p.2310.
[229] T. Mieno, T. Kamo, D. Hayashi, T. Shoji and K. Kadota, Appl. Phys. Lett. 69 (1996) p.617.
[230] A. Granier, F. Nicolazo, C. Val'ee, A. Goullet, G. Turban and B. Grolleau, Plasma Sources Sci. Technol. 6 (1997) p.147.
[231] G.R. Tynan, A.D. Bailey III, G.A. Campbell, R. Charatan, A. de Chambrier, G. Gibson, D.J. Hemker, K. Jones, A. Kuthi, C. Lee, T. Shoji and M. Wilcoxson, J. Vac. Sci. Technol. A 15 (1997) p.2885.
[232] W. Li, Y. Ruan, B. Luther-Davies, A. Rode and R. Boswell, J. Vac. Sci. Technol. A 23 (2006) p.1626.
[233] K. Sadaki, H. Kokubo, D. Hayashi and K. Kadota, Thin Solid Films 386 (2001) p.243.
[234] T. Shima, J. Kim, J. Tominaga and N. Atoda, J. Vac. Sci. Technol. A 19 (2001) p.826.
[235] O. Sarra-Bournet, C. Charles and R. Boswell, Surf. Coat. Technol. 205 (2001) p.3939.
[236] W. Yu, X. Wang, C. Geng, X. Lve, W. Lu and G. Fu, Appl. Surface Sci. 258 (2011) p.1733.
[237] M.J. Baldwin, T.C. Lynch, R.P. Doerner and J.H. Yu, J. Nucl. Mater. 415 (2011) p.S104.
[238] C.K. Birdsall and A.B. Langdon, *Plasma Physics via Computer Simulation*, McGraw-Hill, New York, NY, 1985.
[239] Z. Yoshida, Y. Ogawa, J. Morikawa, S. Watanabe, Y. Yano, S. Mizumaki, T. Tosaka, Y. Ohtani, A. Hayakawa and M. Shibui, Plasma Fusion Res. 1 (2006) p.008.
[240] T. Uchida and S. Hamaguchi, J. Phys. D: Appl. Phys. 41 (2008) p.083001 (Topical Review), and references therein.
[241] V. Vdovin, Plasma Phys. Rep. 39 (2013) p.95.

[242] M. Yamada, R. Kulsrud and H. Ji, Rev. Mod. Phys. 82 (2010) p.603.
[243] P.K. Shukla and B. Eliasson, Rev. Mod. Phys. 81 (2009) p.25 (review paper), and references therein.
[244] M. Miyoshi, Y. Katoh, T. Nishiyama, T. Sakanoi, K. Asamura, M. Hirahata and J. Geophys, Res. 115 (2010) p.A10312 (Aurora, whistler).
[245] R. Treumann and T.E.X. Bernold, Phys. Rev. Lett. 47 (1981) p.1455.
[246] P.W. Schuck, J.W. Bonnell and P.M. Kintner, IEEE Trans Plasma Sci. 31 (2003) p.1125 (review paper), and references therein.
[247] K.M. Lemmer, A.D. Gallimore and T.B. Smith, Plasma Sources Sci. Technol. 18 (2009) p.025019.
[248] , W. Manheimer, L.E. Sugiyama and T.H. Stix, eds., *Plasma Science and the Environment*, American Institute of Physics, New York, 1997.
[249] M.G. Kong, G. Kroesen, G. Morfill, T. Nosenko, T. Shimizu, J. van Dijk and J.L. Zimmermann, New J. Phys. 11 (2009) p.115012 (introductory review paper), and references therein.
[250] http://stw.mext.go.jp/series.html, "Plasma" (in Japanese but English version is also available).